Inorg. Chem. **2008**, *47*, 281–296

Halogen Exchange and Scrambling between C–X and M–X′ Bonds in Copper, Nickel, and Cobalt Complexes of 6,6′-bis(bromo/ chloromethyl)-2,2′-bipyridine. Structural, Electrochemical, and Photochemical Studies

Meenakshi Ghosh,[†] Papu Biswas,[†] Ulrich Flörke,*[,‡] and Kamalaksha Nag*[,†]

Department of Inorganic Chemistry, Indian Association for the Cultivation of Science, Jadavpur, Kolkata 700032, India, and Anorganische und Analytische Chemie, Universität Paderborn, D-33098 , Paderborn, Germany

Received July 25, 2007

The synthesis, reactivities, spectroscopic, electrochemical, and structural studies of copper(I), copper(II), nickel(II), and cobalt(II) complexes of 6,6′-bis(bromomethyl)-2,2′-bipyridine (bpy-Br_2) and 6,6′-bis(chloromethyl)-2,2′-bipyridine (bpy-Cl_2) have been reported. The copper(I) complex $[Cu^{I}(bpy\text{-}Br_2)_2](ClO_4)$ (**1**) has been obtained in two crystallographic modifications, in which the coordination geometry of the metal center has the D_{2d} symmetry. The reaction between $CuCl_2 \cdot 2H_2O$ and bpy-Br_2 has been followed spectrophotometrically at 45 °C over a period of 7 h, and a mechanism for the intramolecular halogen exchange and scrambling in the initially formed compound $[Cu^{II}(bpy\text{-}Br_2)Cl_2]$ (**5**) has been proposed. Depending upon the reaction conditions, several halogen-exchanged products, namely $[Cu^{II}(bpy\text{-}Br_{1.86}Cl_{0.14})(Cl_{1.89}Br_{0.11})]$ (**2**), $[Cu^{II}(bpy\text{-}Br_{1.81}Cl_{0.19})(Cl_{1.70}Br_{0.30})(H_2O)]$ (**3**), and $[Cu^{II}(bpy\text{-}Br_{0.63}Cl_{1.37})(Cl_{0.54}Br_{1.46})]$ (**4**), have been isolated in crystalline form. The reaction between bpy-Cl_2 and $CuCl_2 \cdot 2H_2O$ provides $[Cu^{II}(bpy\text{-}Cl_2)Cl_2]$ (**7**) and $[Cu^{II}(bpy\text{-}Cl_2)Cl_2(H_2O)]$ (**8**), whereas $CoCl_2 \cdot 6H_2O$ and $NiCl_2 \cdot 6H_20$ on reaction with bpy-Br_2 under boiling condition produce $[Co^{II}(bpy\text{-}Br_{0.5}Cl_{1.5})(ClBr)]$ (**11**) and $[Ni^{II}(bpy\text{-}Br_{0.46}Cl_{1.54})(Cl_{0.73}Br_{1.27})(H_2O)]$ (**12**), respectively. The X-ray structures determined for the 4-coordinate compounds **2**, **4**, and **7** show flattened tetrahedral geometry for the metal center with the D_2 symmetry. Both 5-coordinate compounds **3** and **12** have square pyramidal geometry, and whereas the nickel(II) complex **12** has near-perfect geometry ($\tau = 0.015$), considerable distortion is observed for the copper(II) complex **3** ($\tau = 0.25$). Complexes $[Cu^{II}(bpy\text{-}Cl_2)Br_2]$ (**6**) and $[Cu^{II}(bpy\text{-}Br_2)Br_2]$ under boiling condition undergo photoreduction to produce the dimeric copper(I) complexes $[\{Cu^{I}(bpy\text{-}Cl_{1.30}Br_{0.70})(\mu\text{-}Br)\}_2]$(**9**) and $[\{Cu^{I}\text{-}(bpy\text{-}Br_2)(\mu\text{-}Br)\}_2]$ (**10**), respectively. The fact that the photoreduction of $[Cu^{II}(bpy\text{-}Cl_2)Br_2]$ (**6**) and $[Cu^{II}(bpy\text{-}Br_2)Br_2]$ do not take place in absence of light has been established by spectrophotometric measurements. The crystal structures of **9** and **10** have been determined. The electrochemical behavior of all the copper complexes **1**–**10** has been studied in acetonitrile and dichloromethane. The $E_{1/2}$ values for the Cu^{I}/Cu^{II} redox couples show strong solvent dependence and for a given system the $E_{1/2}$ value is more positive in dichloromethane relative to that in acetonitrile. For the compounds $[Cu^{II}(bpy\text{-}Br_{2-x}Cl_x)(Cl_{2-y}Br_y)]$ ($x = 0$–2, $y = 0$–2), the $E_{1/2}$ values become more positive with the increase of y value.

Introduction

As the archetype of polypyridine ligands, 2,2′-bipyridine (bpy), 1,10-phenanthroline (phen), and their derivatives provide a large pool of transition metal complexes that exhibit diversity in stereochemistry, redox activity, photophysical, and other physicochemical properties.[1−10] The low-lying π^* antibonding orbitals of these ligands can accept dπ electron from the low-spin metal centers such as iron(II), ruthenium(II), osmium(II), rhenium(I), and copper(I) to display strong ligand-to-metal charge transfer (LMCT) transition and that forms the basis of studying their ground and excited-state properties. The observation that the copper-

* To whom correspondence should be addressed: E-mail: ickn@iacs.res.in.
[†] Indian Association for the Cultivation of Science.
[‡] Universität Paderborn.

10.1021/ic7014786 CCC: $40.75
Published on Web 12/05/2007

(I) complex $[Cu(dmp)_2]^+$ (dmp = 2,9-dimethyl-1,10-phenanthroline) exhibits luminescence at room temperature, while for the analogue $[Cu(phen)_2]^+$, no photoemission is observed even at 77 K has led[11] to extensive studies[12−23] to find out the structural requirements for copper(I) complexes to exhibit photoluminescence. It is now understood that bulky substituents in the 2- and 9- positions of the phenanthroline ring substantially increase quantum yield and lifetime of copper(I) complexes. The role of these substituents is to inhibit flattening of tetrahedral geometry[16,21,24] in the excited-state which, in turn, prevents quenching through solvent-coordinated exciplex formation.[25,26] In a broader context, correlation between structural parameters and physical properties in copper(I) and copper(II) complexes have been subjected to close scrutiny by several methodologies such as, continuous symmetry measurement,[27] symmetry deformation coordinates and principal component analysis,[28] and structural pathway analysis.[29,30] The redox potential of $[Cu^I(N-N)_2]^+/[Cu^{II}(N-N)_2]^{2+}$ systems show strong dependence on the extent of structural changes that takes place due to electron transfer and the coordinating ability of solvent to the copper(II) center.[20,31−34] Accordingly, stereochemical change plays an important role in determining the kinetics and thermodynamics of redox reactions[35] involving the copper center of polypyridine complexes. Although stereoelectronic influences on various physicochemical properties, including DNA intercalation and nuclease activity,[16,36] have been extensively studied with 2,9- and other ring substituted derivatives of 1,10-phenanthroline copper complexes, similar studies with sterically demanding 6,6′-disubstituted 2,2′-bipyridine systems[35,37−40] have not been carried out to the same extent.

The C−C coupling reactions mediated by copper are of considerable use in organic synthesis.[41] In particular, copper(I) bipyridine complexes have been used as catalysts for atom transfer reactions.[42,43] More recently, halogen atom transfer radical polymerization involving $Cu^IX(bpy)/Cu^{II}X_2(bpy)$ redox cycle has emerged as a major development in controlled radical polymerization process.[44,45] In this process, the homolytic cleavage of an alkyl halide R−X by a copper(I) bipyridine complex produces the alkyl radical R•, which propagates by adding to the double bond of a monomer. The reaction terminates through deactivation when the corresponding copper(II) complex is produced in sufficient concentration. The mechanism of carbon−halogen bond activation by copper(I) and the formation of the halogen atom transferred copper(II) complex have been studied with model systems.[46−48]

In the present study, we are concerned with the structure, stereochemistry, electrochemistry, and reactivities of copper(I) and copper(II) complexes of the ligands 6,6′-bis(bromomethyl)-2,2′-bipyridine (bpy-Br_2) and 6,6′-bis(chloromethyl)-2,2′-bipyridine (bpy-Cl_2) in combination with chloride, bromide, and perchlorate ions. Although exchange reactions are common for the elements of groups 12−17[49] and the reactions involving halides of metallic and nonmetallic

(1) Juris, A.; Balzani, V.; Barigelletti, F.; Campagna, S.; Besler, P.; Zelewsky, A. V. *Coord. Chem. Rev.* **1988**, *84*, 85.
(2) Meyer, T. Z. *Acc. Chem. Res.* **1989**, *22*, 163.
(3) Sammes, P. G.; Yahioglu, G. *Chem. Soc. Rev.* **1994**, *23*, 327.
(4) Kalyansundaram, K. *Photochemistry of Polypyridine and Porphyrin Complexes*; Academic Press: London, 1997.
(5) Bozec, H. L.; Renouard, T. *Eur. J. Inorg. Chem.* **2000**, 229.
(6) Gao, F. G.; Bard, A. J. *J. Am. Chem. Soc.* **2000**, *122*, 7426.
(7) Armaroli, N. *Chem. Soc. Rev.* **2001**, *30*, 113.
(8) Willet, R. D.; Pon, G.; Nagy, C. *Inorg. Chem.* **2001**, *40*, 4342.
(9) Newkome, G. R.; Patri, A. K.; Holder, E.; Schubert, U. *Eur. J. Org. Chem.* **2004**, 235.
(10) Nazeeruddin, M. K.; Klein, C.; Liska, P.; Grätzel, M. *Coord. Chem. Rev.* **2005**, *249*, 1460.
(11) Blaskie, M. W.; McMillin, D. R. *Inorg. Chem.* **1980**, *19*, 3519.
(12) McMillin, D. R.; Kirchoff, J. R.; Goodwin, K. V. *Coord. Chem. Rev.* **1985**, *64*, 83.
(13) Kutal, C. *Coord. Chem. Rev.* **1990**, *99*, 213.
(14) Horvath, O. *Coord. Chem. Rev.* **1994**, *135/136*, 303.
(15) Horvath, A.; Stevenson, K. L. *Coord. Chem. Rev.* **1996**, *153*, 57.
(16) McMillin, D. R.; McNett, K. M. *Chem. Rev.* **1998**, *98*, 1201.
(17) Ruthosky, M.; Kelly, C. A.; Castellano, F. N.; Meyer, G. J. *Coord. Chem. Rev.* **1998**, *171*, 309.
(18) (a) Miller, M. T.; Gantzel, P. K.; Karpisin, T. B. *Inorg. Chem.* **1998**, *37*, 2285. (b) Miller, M. T.; Gantzel, P. K.; Karpisin, T. B. *Inorg. Chem.* **1999**, *38*, 3414.
(19) Cunningham, C. T.; Cunningham, K. L. H.; Michalec, J. F.; McMillin, D. R. *Inorg. Chem.* **1999**, *38*, 4388.
(20) Scaltrito, D. V.; Thompson, D. W.; O'Callaghan, J. A.; Meyer, G, J. *Coord. Chem. Rev.* **2000**, *208*, 243.
(21) Armaroli, N. *Chem. Soc. Rev.* **2001**, *30*, 113.
(22) Cody, J.; Dennisson, J.; Gilmore, J.; VanDerveer, D. G.; Henary, M. M.; Grabielli, A.; Sherril, C. D.; Zhang, Y.; Pan, C. −P.; Burda, C.; Fahrni, C. J. *Inorg. Chem.* **2003**, *42*, 4918.
(23) Kalsani, V.; Schmittel, M.; Listorti, A.; Accorsi, G.; Armaroli, N. *Inorg. Chem.* **2006**, *45*, 2061.
(24) Cunningham, C. T.; Moore, J. T.; Cunningham, K. L. H.; Fanwick, P. E.; McMillin, D. R. *Inorg. Chem.* **2000**, *39*, 3638.
(25) Dietrich-Buchecker, C. O.; Marnot, P. A.; Sauvage, J. P.; Kirchoff, J. R.; McMillin, D. R. *J. Chem. Soc., Chem. Commun.* **1983**, 513.
(26) Gushurst, A. K. I.; McMillin, D. R.; Dietrich-Buchecker, C. O.; Sauvage, J. P. *Inorg. Chem.* **1989**, *28*, 4070.
(27) (a) Keinan, S.; Avnir, D. *Inorg. Chem.* **2001**, *40*, 318. (b) Keinan, S.; Avnir, D. *J. Chem. Soc., Dalton Trans.* **2001**, 941.
(28) Raithby, P. R.; Schields, G. P.; Allen, F. H.; Motherwell, W. D. S. *Acta Crystallogr.* **2000**, *B56*, 444.
(29) O'Sullivan, C.; Murphy, G.; Murphy, B.; Hatahway, B. J. *J. Chem. Soc., Dalton Trans.* **1999**, 1835.
(30) Burgi, H.; Dunitz, J. D. *Acc. Chem. Res.* **1983**, *16*, 153.
(31) James, B. R.; Williams, R. J. P. *J. Chem. Soc.* **1961**, 2007.
(32) Federlin, P.; Kern, J. −M.; Rastegar, A.; Dietrich-Buchecker, C. O.; Marnot, P. A.; Sauvage, J. P. *New. J. Chem.* **1990**, *14*, 9.
(33) Eggelston, M. K.; McMillin, D. R.; Koenig, K. S.; Pallenberg, A. J. *Inorg. Chem.* **1997**, *36*, 172.
(34) Miller, M. T.; Karpishin, T. B. *Inorg. Chem.* **1999**, *38*, 5246.
(35) (a) Koshino, N.; Kuchiyama, Y.; Ozaki, H.; Funahasi, S.; Takagi, H. D. *Inorg. Chem.* **1999**, *38*, 3352. (b) Itoh, S.; Kishikawa, N.; Suzuki, T.; Takagi, H. D. *Dalton Trans.*. **2005**, 1066.
(36) Pogozeleski, W. K.; Tullius, T. D.; *Chem. Rev.* **1998**, *98*, 1089.
(37) Burke, P. J.; Henrick, K.; McMillin, D. R. *Inorg. Chem.* **1982**, *21*, 1881.
(38) Williams, R. M.; Cola, L. D.; Hartl, F.; Lagref, J.-J.; Planeix, J.-M.; Cian, A. D.; Hosseini, M. W. *Coord. Chem. Rev.* **2002**, *230*, 253.
(39) Siddique, Z. A.; Yamomoto, Y.; Ohno, T.; Nozaki, K. *Inorg. Chem.* **2003**, *42*, 6366.
(40) Kume, S.; Kurihara, M.; Nishihara, H. *Inorg. Chem.* **2003**, *42*, 2194.
(41) Hassan, J.; Sevignon, M.; Gozzi, C.; Schulz, E.; Lemaire, M. *Chem. Rev.* **2002**, *102*, 1359.
(42) Minisci, F. *Acc. Chem. Res.* **1975**, *8*, 165.
(43) Curran, D. P. *Synthesis*, **1988**, 489.
(44) Patten, T. E.; Matyiaszewski, K. *Acc. Chem. Res.* **1999**, *32*, 895.
(45) Matyiaszewski, K.; Xia, J. H. *Chem. Rev.* **2001**, *101*, 2921.
(46) Pintauer, T.; Qiu, J.; Kickelbick, G.; Matyiaszewski, K. *Inorg. Chem.* **2001**, *40*, 2818.
(47) Levy, A. T.; Olmstead, M. M.; Pattern, T. E. *Inorg. Chem.* **2000**, *39*, 1628.
(48) Osako, T.; Karlin, K. D.; Itoh, S. *Inorg. Chem.* **2005**, *44*, 410.
(49) Lockhart, J. C. *Chem. Rev.* **1965**, *65*, 131.

elements have been widely studied,[50] to our knowledge, exchange reaction between carbon−halogen and metal−halogen bonds are quite uncommon. We report here that the tetracoordinate copper(II) complex $[Cu^{II}(bpy\text{-}Br_2)Cl_2]$, undergoes halogen exchange and scrambling to produce $[Cu^{II}(bpy\text{-}Br_{2-x}Cl_x)Cl_{2-y}Br_y]$ complexes. Further, $[Cu^{II}(bpy\text{-}Cl_2)Br_2]$ undergoes photoreduction to produce the dimeric copper(I) complex $[\{Cu^{I}(bpy\text{-}Cl_{2-x}Br_x)(\mu\text{-}Br)\}_2]$.

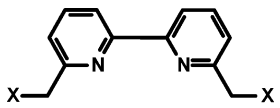

X = Br; bpy-Br_2
X = Cl; bpy-Cl_2

Experimental Section

Materials. Reagent grade chemicals obtained from commercial sources were used as received. Solvents were purified and dried according to standard methods.[51] 6,6′-bis(bromomethyl)-2,2′-bipyridine (bpy-Br_2)[52] and 6,6′-bis(chloromethyl)-2,2′-bipyridine (bpy-Cl_2)[53] were prepared according to the literature methods.

Caution! The halomethyl bipyridines are highly lachrymatory and care should be exercised to avoid contact with skin and nose. All the perchlorate salts reported in this study are potentially explosive and therefore should be handled with care.

Preparation of the Complexes. $[Cu^{I}(bpy\text{-}Br_2)_2](ClO_4)$ (1a, 1b). This compound was obtained in two different crystallographic modifications by using the following two methods.

Method A. To a solution of bpy-Br_2 (0.342 g, 1 mmol) in chloroform (20 mL) a suspension of $[Cu(CH_3CN)_4](ClO_4)$ (0.164 g, 0.5 mmol) in acetonitrile (5 mL) was added under nitrogen atmosphere. The mixture was stirred at room temperature for 1 h, during which time a clear deep red solution was obtained. On slow evaporation of the solution, bright red crystals that deposited were collected by filtration and washed with ethanol and diethyl ether; yield: 0.38 g (90%). ESI−MS (acetonitrile): m/z = 746.3 (15%) $[Cu(bpy\text{-}Br_2)_2]^+$; 404.6 (100%) $[Cu(bpy\text{-}Br_2)]^+$. Anal. Calcd for $C_{24}H_{20}Br_4ClCuN_4O_4$: C, 34.00; H, 2.36; N, 6.61. Found: C, 33.96; H, 2.48; N, 6.56. FT-IR (KBr, cm^{-1}): 3430br, 3101w, 3038w, 2933w, 1595 m, 1570 m, 1463 m, 1433 m, 1208w, 1089s, 801 m, 748 m, 629 m, 592w. ^1H NMR (CD_3CN): 8.42(d, J = 8.0 Hz, 2H, Ar−H), 8.16(t, J = 7.9 Hz, 2H, Ar−H), 7.76(d, J = 7.7 Hz, 2H, Ar−H), 4.39(s, 4H, CH_2). UV−vis[CH_2Cl_2, λ_{max}/nm(ϵ/$M^{-1}cm^{-1}$)]: 270(37 000), 310(44 000), 450(7 800).

Method B. To a solution of bpy-Br_2 (0.342 g, 1 mmol) in chloroform (20 mL) a methanol solution (10 mL) of $Cu(ClO_4)_2\cdot 6H_2O$ (0.185 g, 0.5 mmol) was added and the mixture was stirred at room temperature for 1 h. The color of the solution changed from green to greenish yellow and finally to orange red. On evaporation of the solution, a mixture containing predominantly red crystals and some greenish yellow crystals were obtained. The red crystals were extracted with chloroform, filtered, and the filtrate on slow evaporation deposited diffraction quality crystals; yield: 0.25 g (60%). ESI−MS (acetonitrile): m/z = 746.3 (15%) $[Cu(bpy\text{-}Br_2)_2]^+$; 404.6 (100%) $[Cu(bpy\text{-}Br_2)]^+$. Anal. Calcd for $C_{24}H_{20}Br_4ClCuN_4O_4$: C, 34.00; H, 2.36; N, 6.61. Found: C, 34.08; H, 2.33; N, 6.52. FT-IR (KBr, cm^{-1}): 3443br, 3098w, 3038w, 2926w, 1596 m, 1572 m, 1462 m, 1430 m, 1206 m, 1087s, 844w, 805 m, 749 m, 631 m, 582w. ^1H NMR (CD_3CN): 8.42(d, 2H, Ar−H), 8.16(t, 2H, Ar−H), 7.76(d, 2H, Ar−H), 4.39(s, 4H, CH_2). UV−vis[CH_2Cl_2, λ_{max}/nm (ϵ/ $M^{-1}cm^{-1}$)]: 270(37 000), 310(44 000), 450(7 800).

The greenish yellow compound (0.1 g, 30% yield) was characterized as $[Cu(bpy\text{-}Br_2)(H_2O)_3](ClO_4)_2$. Anal. Calcd for $C_{12}H_{16}Br_2Cl_2CuN_2O_{11}$: C, 21.88; H, 2.43; N, 4.25. Found: C, 22.21; H, 2.57; N, 4.16. FT-IR (KBr, cm^{-1}): 3450br, 3260s, 3116w, 3048w, 2926w, 1598s, 1570s, 1461 m, 1432 m, 1245 m, 1194 m, 1090s, 802 m, 751 m, 630 m, 590w.

$[Cu^{II}(bpy\text{-}Br_{1.86}Cl_{0.14})(Cl_{1.89}Br_{0.11})]$ (2). To a solution of $CuCl_2\cdot 2H_2O$ (0.171 g, 1 mmol) in methanol (10 mL) was added a chloroform solution (20 mL) of bpy-Br_2 (0.342 g, 1 mmol). The solution was filtered and allowed to stand at room temperature for 2 h. The red crystals that deposited during this period were filtered and washed with diethyl ether; yield: 0.20 g (40%). Anal. Calcd for $C_{12}H_{10}Br_{1.97}Cl_{2.03}Cu\ N_2$: C, 30.33; H, 2.11; N, 5.90. Found: C, 29.96; H, 2.21; N, 5.79. FT-IR (KBr, cm^{-1}): 3398br, 3020w, 2902w, 1597s, 1568s, 1462 m, 1431s, 1275 m, 1244 m, 1188 m, 1105 m, 1007w, 791 m, 748 m, 671 m, 588w. UV−vis[CH_3CN, λ_{max}/nm (ϵ/$M^{-1}cm^{-1}$)]: 255(14 200), 315(24 900), 440(870), 845-(90), 990(75).

$[Cu^{II}(bpy\text{-}Br_{1.81}Cl_{0.19})(Cl_{1.70}Br_{0.30})(H_2O)]$ (3). The filtrate after the separation of **2** on standing for overnight period deposited a green crystalline compound. This was filtered and washed with ethanol and diethyl ether; yield: 0.22 g (45%). Anal. Calcd for $C_{12}H_{12}Br_{2.11}Cl_{1.89}CuN_2O$: C, 28.92; H, 2.41; N, 5.62. Found: C, 28.76; H, 2.51; N, 5.54. FT-IR (KBr, cm^{-1}): 3255 s, br, 3157w, 3065 m, 2957 m, 1593s, 1572s, 1464 m, 1428s, 1268 m, 1243w, 1211 m, 1179 m, 1103w, 1008 m, 807s, 752 m, 609 m, 550w. UV−vis[CH_3CN, λ_{max}/nm (ϵ/$M^{-1}cm^{-1}$)]: 255(14 400), 315(25 100), 435(940), 845(100), 975(90).

$[Cu^{II}(bpy\text{-}Br_{0.63}Cl_{1.37})(Cl_{0.54}Br_{1.46})]$ (4). A chloroform solution (25 mL) of bpy-Br_2 (0.342 g, 1 mmol) and a methanol solution (10 mL) $CuCl_2\cdot 2H_2O$ (0.171 g, 1 mmol) were mixed together and heated under reflux for 2 h. The solution was then concentrated to ~5 mL and kept in a closed container. After several hours the maroon crystals that deposited were filtered and washed with ethanol and diethyl ether; yield: 0.38 g (80%). Anal. Calcd for $C_{12}H_{10}Br_{2.09}Cl_{1.91}CuN_2$: C, 30.00; H, 2.08; N, 5.83. Found: C, 29.74; H, 2.24; N, 5.69. FT-IR (KBr, cm^{-1}): 3257 br, 3145 m, 3066 m, 2939w, 1591s, 1570 m, 1464s, 1427s, 1269 m, 1210w, 1180w, 1143w, 1008w, 805s, 755 m, 685 m, 645w, 605w. UV−vis[CH_3CN, λ_{max}/nm (ϵ/$M^{-1}cm^{-1}$)]: 255(14 300), 315(25 000), 430-(1000), 580(sh), 640(sh), 875(115), 1090(100).

$[Cu^{II}(bpy\text{-}Br_2)Cl_2]$ (5). A methanol solution (10 mL) of $CuCl_2\cdot 2H_2O$ (0.171 g, 1 mmol) and a chloroform solution (20 mL) of bpy-Br_2 (0.342 g, 1 mmol) were mixed together and the resulting solution was immediately flash-evaporated to dryness at room temperature. The residue was stirred with chloroform and filtered. The solid remaining was then dissolved in dichloromethane and filtered. The filtrate was quickly evaporated to dryness at room temperature under vacuum; yield: 0.24 g (80%). Anal. Calcd for $C_{12}H_{10}Br_2Cl_2CuN_2$: C, 30.22; H, 2.10; N, 5.88. Found: C, 30.12; H, 2.19; N, 5.76. FT-IR (KBr, cm^{-1}): 3265 br, 3068 m, 3026 m,

(50) (a) Van Wazer, J. R.; Moedritzer, K. *J. Am. Chem. Soc.* **1966**, *88*, 547. (b) Riess, J. G; Elkaim, J. −C. Pace, S. C. *Inorg. Chem.* **1973**, *12*, 2874. (c) Garralda, M.; Garcia, V.; Kretschmer, M.; Pregosin, P. S.; Ruegger, H. *Hel. Chim. Acta.* **1981**, *64*, 1150. (d) Orvik, J. A. *J. Org. Chem.* **1996**, *61*, 4933.
(51) Perrin, D. D.; Armarego, W. L.; Perrin, D. R. *Purification of Laboratory Chemical*, 2nd ed.; Pergamon Press: Oxford, 1980.
(52) Rodriguez-Ubis, J.-C.; Alpha, B.; Plancherel, D.; Lehn, J.-M. *Hel. Chim. Acta.* **1984**, *67*, 2264.
(53) Newkome, G. R.; Puckett, W. E.; Kiefer, G. E.; Gupta, U. K.; Xia, Y.; Coreil, M.; Hackney, M. A. *J. Org. Chem.* **1982**, *47*, 4116.

1593s, 1571 m, 1462s, 1427 m, 1275 m, 1247 m, 1178 m, 1134w, 1010 m, 802s, 750 m, 644 m, 607 m. UV−vis[CH_3CN, λ_{max}/nm (ϵ/$M^{-1}cm^{-1}$)]: 255(14 000), 315(24 000), 445(820), 850(95), 1000-(75).

[Cu^{II}(bpy-Cl_2)Br_2] (6). This dark brown compound was prepared in the same way as **5**, with the difference that a methanol solution of $CuBr_2$ (0.23 g, 1 mmol) and a chloroform solution of bpy-Cl_2 (0.25 g, 1 mmol) were used as the reactants; yield: 0.24 g (80%). Anal. Calcd for $C_{12}H_{10}Br_2Cl_2CuN_2$: C, 30.22; H, 2.10; N, 5.88. Found: C, 30.16; H, 2.18; N, 5.83. FT-IR (KBr, cm^{-1}): 3463br, 3086 m, 2945 m, 1597s, 1568 m, 1463s, 1425 m, 1274 m, 1252 m, 1182 m, 1161 m, 1020 m, 802s, 754s, 706 m, 646 m. UV−vis[CH_3CN, λ_{max}/nm (ϵ/$M^{-1}cm^{-1}$)]: 255(14 500), 310(25 000), 425-(1100), 570(sh), 630(sh), 880(125), 1080(100).

[Cu^{II}(bpy-Cl_2)Cl_2] (7) and **[Cu^{II}(bpy-Cl_2)Cl_2(H_2O)] (8).** A mixture of bpy-Cl_2 (0.25 g, 1 mmol) in chloroform (10 mL) and $CuCl_2 \cdot 2H_2O$ (0.17 g, 1 mmol) in methanol (5 mL) was stirred for 0.5 h, after which the solution was kept undisturbed for 2 h. During this period, red crystals began to separate out from the solution. The product was collected by filtration and it was characterized as **7**. The filtrate was again kept undisturbed in a closed container for several hours, during which period an additional crop of a mixture of red and green crystals were deposited. After filtration, the filtrate was allowed to evaporate slowly when only the green crystals deposited. The product (**8**) was filtered off and washed with dichloromethane to remove any cocrystallized compound **7**.

7: Anal. Calcd for $C_{12}H_{10}Cl_4CuN_2$: C, 37.15; H, 2.59; N, 7.22. Found: C, 36.98; H, 2.65; N, 7.13. FT-IR (KBr, cm^{-1}): 3252br, 3080w, 3016 m, 2949 m, 1597s, 1570 m, 1464s, 1441 m, 1427 m, 1276 m, 1254w, 1184 m, 1163 m, 1112w, 835 m, 804s, 756 m, 707 m, 640 m. UV−vis[CH_3CN, λ_{max}/nm (ϵ/$M^{-1}cm^{-1}$)]: 250(10 800), 310(15 000), 440(750), 860(100), 1050(70).

8: Anal. Calcd for $C_{12}H_{12}Cl_4CuN_2O$: C, 35.51; H, 2.96; N, 6.90. Found: C, 35.62; H, 3.04; N, 6.81. FT-IR (KBr, cm^{-1}): 3254br, 3169 m, 3069 m, 2951 m, 1595s, 1573s, 1466s, 1429s, 1269s, 1182 m, 1148 m, 1107 m, 1026 m, 1009 m, 835 m, 808s, 758s, 710s, 648 m, 605w, 563w. UV−vis[CH_3CN, λ_{max}/nm (ϵ/$M^{-1}cm^{-1}$)]: 250-(10 900), 310(15 100), 440(815), 850(75), 970(70).

[{Cu^{I}(bpy-$Cl_{1.30}Br_{0.70}$)(μ-Br)}$_2$](9). To a boiling chloroform solution (20 mL) of bpy-Cl_2 (0.25 g, 1 mmol) was added a methanol solution (10 mL) of $CuBr_2$ (0.23 g, 1 mmol). The resulting dark red solution was refluxed for 4 h. On concentration of the solution to ~10 mL, a light brown crystalline product was obtained, which was filtered and washed with 1:1 ethanol/diethyl ether mixture; yield: 0.18 g (42%). Anal. Calcd for $C_{24}H_{20}Br_{3.40}Cl_{2.60}Cu_2N_4$: C, 33.67; H, 2.34; N, 6.55. Found: C, 33.46; H, 2.43; N, 6.42. FT-IR (KBr, cm^{-1}): 3462br, 1634 m, 1595s, 1458 m, 1424s, 1271 m, 1220 m, 1166 m, 1096 m, 1007 m, 775s, 746 m, 671 m. ^{1}H NMR (CD_3CN): 8.40(d, J = 8.1 Hz, 2H, Ar−H), 8.11(t, J = 8.0 Hz, 2H, Ar−H), 7.80(d, J = 7.7 Hz, 2H, Ar−H), 4.70(s, 4H, CH_2). UV−vis[CH_3CN, λ_{max}/nm (ϵ/$M^{-1}cm^{-1}$)]: 250(32 000), 315(57 500), 440(2 900).

[{Cu^{I}(bpy-Br_2)(μ-Br)}$_2$] (10). This compound was prepared in the same way as **9**, by boiling a mixture of bpy-Br_2 (0.34 g, 1 mmol) in chloroform (15 mL) and $CuBr_2$ (0.23 g, 1 mmol) in methanol (10 mL) for 4 h; yield: 0.39 g (80%). Anal. Calcd for $C_{24}H_{20}Br_6Cu_2N_4$: C, 29.66; H, 2.06; N, 5.77. Found: C, 29.61; H, 2.12; N, 5.72. FT-IR (KBr, cm^{-1}): 3464br, 3085 m,1641 m, 1595s, 1570 m, 1460 m, 1431s, 1273 m, 1213 m, 1176 m, 1006 m, 793s, 746 m, 639 m, 59 m. ^{1}H NMR (CD_3CN): 8.40(d, J = 8.2 Hz, 2H, Ar−H), 8.11(t, J = 8.0 Hz, 2H, Ar−H), 7.80(d, J = 7.6 Hz, 2H, Ar−H), 4.53(s, br, 4H, CH_2). UV−vis[CH_2Cl_2, λ_{max}/nm (ϵ/$M^{-1}cm^{-1}$)]: 250(32 500), 315(58 000), 440(2 600).

[Co^{II}(bpy-$Br_{0.5}Cl_{1.5}$)(ClBr)] (11). To a chloroform solution (20 mL) of bpy-Br_2 (0.342 g, 1 mmol) was added an acetonitrile solution (20 mL) of $CoCl_2 \cdot 6H_2O$ (0.24 g, 1 mmol) and the mixture was heated under reflux for 2 h. The solution was filtered to remove any suspended material and the filtrate was concentrated to a volume of ~10 mL when blue crystals of **11** began to deposit. The product was collected by filtration and washed with ethanol and diethyl ether; yield: 0.38 g, (80%). Anal. Calcd for $C_{12}H_{10}Br_{1.5}Cl_{2.5}CoN_2$: C, 32.04; H, 2.22; N, 6.23. Found: C, 31.90; H, 2.31; N, 6.15. FT-IR (KBr, cm^{-1}): 3216br, 3082 m, 3015 m, 1597s, 1566 m, 1462s, 1433s, 1281 m, 1251w, 1180 m, 1111w, 1022 m, 926w, 905 m, 876w, 837 m, 800s, 754 m, 675 m, 648 m, 607 m, 434w. UV−vis[CH_3CN, λ_{max}/nm (ϵ/$M^{-1}cm^{-1}$)]: 240(11 800), 290(12 150), 320(sh), 575(180), 670(430), 1350(60).

[Ni^{II}(bpy-$Br_{0.46}Cl_{1.54}$)($Cl_{0.73}Br_{1.27}$)(H_2O)] (12). This compound was obtained as olive green crystals in the same way as **11**, with the difference that an acetonitrile solution (20 mL) of $NiCl_2 \cdot 6H_2O$ (0.24 g, 1 mmol) was used instead of $CoCl_2 \cdot 6H_2O$; yield: 0.40 g (85%). Anal. Calcd for $C_{12}H_{10}Br_{1.73}Cl_{2.27}N_2NiO$: C, 30.13; H, 2.51; N, 5.86. Found: C, 30.31; H, 2.67; N, 5.84. FT-IR (KBr, cm^{-1}): 3263s,br, 3060 m, 1597s, 1470s, 1429s, 1327w, 1269s, 1213 m, 1180 m, 1143 m, 1103 m, 1020 m, 939w, 897w, 806s, 754 m, 707 m, 644 m, 613 m, 561 m, 448w. UV−vis[CH_3CN, λ_{max}/nm (ϵ/$M^{-1}cm^{-1}$)]: 240(12 000), 300(11 600), 320(sh), 510(125), 610-(sh), 860(30), 1000(60).

Isolation of the Demetalated Halogen-Exchanged Ligands. The copper(II) complexes [Cu^{II}(bpy-$Br_{1.81}Cl_{0.19}$)($Cl_{1.70}Br_{0...30}$)(H_2O)] (**3**) and [Cu^{II}(bpy-$Br_{0.63}Cl_{1.37}$)($Cl_{0.54}Br_{1.46}$)] (**4**) were demetalated by dissolving the compounds in hot methanol and to which a solution of sodium hydrosulfide in methanol was added in a dropwise manner under vigorously stirred condition. When the precipitation of black copper(II) sulfide was complete, the mixture was allowed to stand for a few minutes and was then filtered. The colorless filtrate was evaporated to dryness on a rotary evaporator and from the residue the modified ligand was extracted with chloroform leaving behind the sodium halides as residue. On evaporation of the solvent the product deposited as white crystalline solid. The recovery of the modified ligands were almost quantitative.

The nickel(II) complex [Ni(bpy-$Br_{0.46}Cl_{1.54}$)($Cl_{0.73}Br_{1.27}$)(H_2O)] (**12**), on boiling with methanol containing one drop of sulfuric acid (M), liberated the ligand quantitatively. The white crystalline product that deposited was collected by filtration after cooling the mixture to room temperature.

bpy-$Br_{1.81}Cl_{0.19}$: Anal. Calcd for $C_{12}H_{10}Br_{1.81}Cl_{0.19}N_2$: C, 43.20; H, 3.00; N, 8.40. Found: C, 42.94; H, 3.09; N, 8.28. ESI-MS (CH_2-Cl_2): m/z = 364.91 (40%) [$C_{12}H_{10}Br_2N_2 + Na^+$]; 342.92 (65%) [$C_{12}H_{10}Br_2N_2 + H^+$]; 320.96 (100%) [$C_{12}H_{10}BrClN_2 + Na^+$]; 298.97 (96%) [$C_{12}H_{10}BrClN_2 + H^+$]; 275.00 (60%) [$C_{12}H_{10}Cl_2N_2 + Na^+$]; 262.99 (39%) [$C_{12}H_{10}BrN_2 + H^+$]; 253.03 (40%) [$C_{12}H_{10}$-$Cl_2N_2 + H^+$]; 219.07 (10%) [$C_{12}H_{10}ClN_2 + H^+$].

^{1}H NMR ($CDCl_3$): 8.40 (m, 2H, Ar−H); 7.85 (m, 2H, Ar−H); 7.50 (m, 2H, Ar−H); 4.75, 4.64 (s, 4H, CH_2Cl : CH_2Br = 0.4 : 3.6).

bpy-$Br_{0.63}Cl_{1.37}$: Anal. Calcd for $C_{12}H_{10}Br_{0.63}Cl_{1.37}N_2$: C, 51.28; H, 3.56; N, 9.96. Found: C, 51.56; H, 4.58; N, 9.90. ESI−MS (CH_2Cl_2): m/z = 364.91 (5%) [$C_{12}H_{10}Br_2N_2 + Na^+$]; 342.92 (23%) [$C_{12}H_{10}Br_2N_2 + H^+$]; 320.96 (33%) [$C_{12}H_{10}BrClN_2 + Na^+$]; 298.97 (95%) [$C_{12}H_{10}BrClN_2 + H^+$]; 275.00 (45%) [$C_{12}H_{10}Cl_2N_2 + Na^+$]; 262.99 (5%) [$C_{12}H_{10}BrN_2 + H^+$]; 253.03 (100%) [$C_{12}H_{10}Cl_2N_2 + H^+$]; 219.07 (5%) [$C_{12}H_{10}ClN_2 + H^+$]. ^{1}H NMR ($CDCl_3$): 8.40

Table 1. Crystallographic Data for Complexes **1**(**a** and **b**), **2**, **3**, **4**, **7**, **9**, **10** and **12**

	1a	**1b**	**2**	**3**
empirical formula	$C_{24}H_{20}Br_4ClCu\ N_4O_4$	$C_{24}H_{20}Br_4ClCu\ N_4O_4$	$C_{12}H_{10}Br_{1.966}Cl_{2\ .034}CuN_2$	$C_{12}H_{12}Br_{2.11}Cl_{1.\ 89}CuN_2O$
Fw	847.07	847.07	474.70	497.87
T, K	150(2)	150(2)	150(2)	150(2)
crystal syst, space group	monoclinic, $P2_1/n$	monoclinic, $P2_1/c$	monoclinic, $P2_1/c$	monoclinic, $P2_1/n$
a, Å	13.6503(7)	16.4933(6)	7.4752(7)	9.7776(12)
b, Å	13.2877(7)	19.9905(8)	15.6725(13)	7.5783(9)
c, Å	15.8870(9)	18.5600(7)	12.6372(11)	20.600(3)
α, deg	90	90	90	90
β, deg	99.757(1)	109.560(1)	103.837(2)	92.811(2)
γ, deg	90	90	90	90
V, Å^3	2839.9(3)	5766.3(4)	1437.5(2)	1524.5(3)
Z, ρ_{calcd}, Mg m^{-3}	4, 1.981	8, 1.951	4, 2.193	4, 2.169
μ, mm^{-1}	6.529	6.431	7.331	7.203
F(000)	1640	3280	913	961
crystal size, mm^3	0.45 0.25 0.20	0.40 0.20 0.04	0.15 0.10 0.08	0.30 0.22 0.10
no. of reflns [$I > 2\sigma(I)$]	18820	35469	10825	9815
no. of data/restraints/ params	5787/0/343	11645/58/702	2942/0/176	3108/13/208
GOF on F^2	1.043	0.797	0.978	0.911
final *R* indices [$I > 2\sigma(I)$]	$R1^a = 0.0339$, $wR2^b = 0.0765$	$R1^a = 0.0452$, $wR2^b = 0.0702$	$R1^a = 0.0485$, $wR2^b = 0.0649$	$R1^a = 0.0250$, $wR2^b = 0.0484$
R indices (all data)	$R1^a = 0.0479$, $wR2^b = 0.0811$	$R1^a = 0.1146$, $wR2^b = 0.0810$	$R1^a = 0.1094$, $wR2^b = 0.0764$	$R1^a = 0.0321$, $wR2^b = 0.0499$

4	**7**	**9**	**12**
$C_{12}H_{10}Br_{2.09}Cl_{1.91}C\ uN_2$	$C_{12}H_{10}Cl_4CuN_2$	$C_{24}H_{20}Br_{3.40}Cl_{2.\ 60}Cu_2N_4$	$C_{12}H_{12}Br_{1.73}Cl_{2.\ 27}N_2NiO$
480.08	387.56	855.38	477.66
150(2)	150(2)	120(2)	120(2)
monoclinic, $P2_1/c$	monoclinic, $P2_1/c$	triclinic, $P\bar{1}$	monoclinic, $P2_1/n$
7.2944(6)	7.2122(5)	8.2536(8)	9.8515(6)
17.1836(15)	16.7929(12)	9.5607(9)	7.6429(5)
11.8504(10)	11.5223(8)	9.8568(10)	20.6049(13)
90	90	67.604(2)	90
95.701(2)	95.977(2)	83.355(2)	93.806(1)
90	90	67.630(2)	90
1478.0(2)	1378.92(17)	664.63(11)	1548.00(17)
4, 2.157	4, 1.855	1, 2.137	4, 2.049
7.445	2.327	6.995	6.105
922	772	413	932
0.40 0.12 0.04	0.21 0.04 0.03	0.18 0.04 0.04	0.37 0.21 0.02
15416	13837	5982	12236
3007/8/207	3301/0/173	3147/4/184	3666/11/223
0.880	0.915	0.857	0.998
$R1^a = 0.0310$, $wR2^b = 0.0531$	$R1^a = 0.0447$, $wR2^b = 0.0832$	$R1^a = 0.0456$, $wR2^b = 0.0976$	$R1^a = 0.0321$, $wR2^b = 0.0836$
$R1^a = 0.0496$, $wR2^b = 0.0565$	$R1^a = 0.1055$, $wR2^b = 0.0948$	$R1^a = 0.1041$, $wR2^b = 0.1783$	$R1^a = 0.0399$, $wR2^b = 0.0874$

^{a} $R1(F) = \Sigma||F_o|-|F_c||/\Sigma|F_o|$. ^{b} $wR2(F^2) = [\Sigma w(F_o^2-F_c^2)^2/\Sigma w(F_o^2)^2]^{1/2}$.

(m, 2H, Ar−H); 7.85 (m, 2H, Ar−H); 7.50 (m, 2H, Ar−H); 4.75, 4.64 (s, 4H, CH_2Cl : CH_2Br = 2.7 : 1.3).

bpy-$Br_{0.46}Cl_{1.54}$: Anal. Calcd for $C_{12}H_{10}Br_{0.46}Cl_{1.54}N_2$: C, 52.70; H, 3.66; N, 10.24. Found: C, 52.48; H, 3.71; N, 10.17. ESI−MS (CH_2Cl_2): *m*/*z* = 364.91 (35%) [$C_{12}H_{10}Br_2\ N_2 + Na^+$]; 342.92 (40%) [$C_{12}H_{10}Br_2\ N_2 + H^+$]; 320.96 (100%) [$C_{12}H_{10}BrClN_2 + Na^+$]; 298.97 (65%) [$C_{12}H_{10}BrClN_2 + H^+$]; 275.00 (40%) [$C_{12}H_{10}Cl_2\ N_2 + Na^+$]; 262.99 (10%) [$C_{12}H_{10}BrN_2 + H^+$]; 253.03 (15%) [$C_{12}H_{10}Cl_2\ N_2 + H^+$]. ^{1}H NMR ($CDCl_3$): 8.39 (m, 2H, Ar−H); 7.85 (m, 2H, Ar−H); 7.49 (m, 2H, Ar−H); 4.75, 4.64 (s, 4H, CH_2Cl : CH_2Br = 3:1).

bpy-Br_2.[52] ESI−MS (CH_2Cl_2): *m*/*z* = 364.92 (100%) [$C_{12}H_{10}Br_2\ N_2 + Na^+$]; 342.97 (50%) [$C_{12}H_{10}Br_2\ N_2 + H^+$]; 263.03 (50%) [$C_{12}H_{10}BrN_2 + H^+$]. ^{1}H NMR ($CDCl_3$): 8.39 (d, *J* = 7.90 Hz, 2H, Ar−H); 7.84 (t, *J* = 7.75 Hz, 2H, Ar−H); 7.48 (d, *J* = 7.65 Hz, 2H, Ar−H); 4.64 (s, 4H, CH_2).

bpy-Cl_2.[53] ESI−MS (CH_2Cl_2): *m*/*z* = 274.99 (100%) [$C_{12}H_{10}Cl_2\ N_2 + Na^+$]; 253.00 (40%) [$C_{12}H_{10}Cl_2\ N_2 + H^+$]; 219.04 (5%) [$C_{12}H_{10}ClN_2 + H^+$]. ^{1}H NMR ($CDCl_3$): 8.40 (d, *J* = 8.0 Hz, 2H, Ar−H); 7.85 (t, *J* = 7.7 Hz, 2H, Ar−H); 7.52 (d, *J* = 7.8 Hz, 2H, Ar−H); 4.75 (s, 4H, CH_2).

Physical Measurements. Elemental (C, H, and N) analyses were performed on a Perkin-Elmer 2400II elemental analyzer. IR spetra were recorded using KBr disks on a Shimadzu FTIR 8400S spectrometer. The electronic absorption spectra were obtained with a Perkin-Elmer 950 UV−vis-NIR spectrophotometer. The electrospray ionization mass spectra (ESI−MS) were measured on a Micromass Qtof YA 263 mass spectrometer. The ^{1}H NMR (300 MHz) spectra were recorded on a Bruker Avance DPX-300 spectrometer. The electrochemical measurements of complexes in acetonitrile and dichloromethane were performed at 25 °C under nitrogen using a Bioanalytical Systems BAS 100B electrochemical analyzer. The supporting electrolyte (0.1 M) was tetrabutylammonium perchlorate (TBAP) and solutions were 10^{-3} M in complexes. Cyclic voltammetric (CV) and Osteryoung square wave voltammetric (OSWV) measurements were carried out with a three-electrode assembly comprising either a platinum or glassy carbon disk working electrode, platinum auxiliary electrode and an aqueous Ag/AgCl reference electrode (290 mV vs NHE). IR compensation was made automatically during each run. Under the experimental conditions used, the $E_{1/2}$ value of the ferrocene/ ferrocenium couple was 420 mV in acetonitrile and 440 mV in dichloromethane.

Crystal Structure Determination of 1(a and b) 2, 3, 4, 7, 9, and 12. The crystals of the above-mentioned compounds were mounted on glass fibers using perfluoropolyether oil. Intensity data were collected on a Bruker AXS SMART APEX diffractometer at

Scheme 1

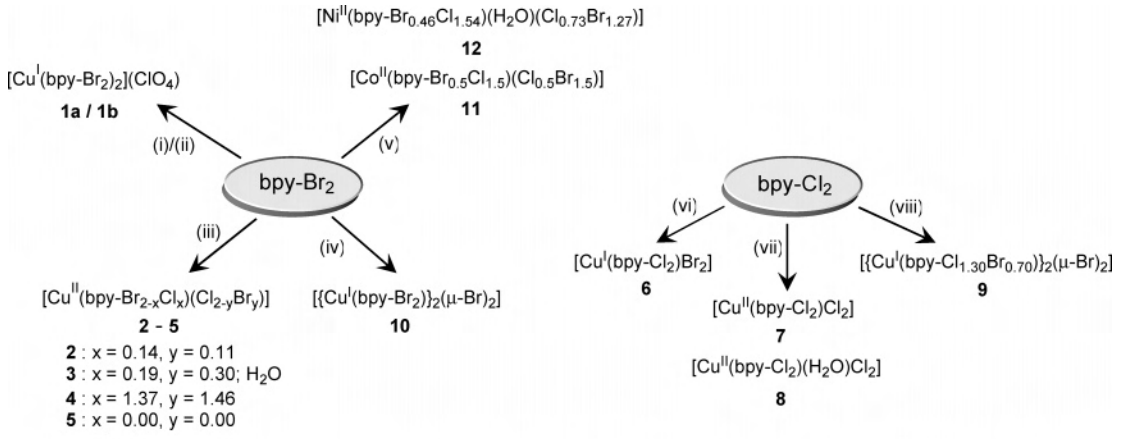

(i) $[Cu^{I}(CH_3CN)_4](ClO_4)$; (ii) $Cu^{II}(ClO_4)_2 \cdot 6H_2O$; (iii) $Cu^{II}Cl_2 \cdot 2H_2O$, at varying reaction time and temperature;(iv) $Cu^{II}Br_2$, reflux; (v) $M^{II}Cl_2 \cdot 6H_2O$ (M = Co, Ni); (vi) $Cu^{II}Br_2$, short reaction time; (vii) $Cu^{II}Cl_2 \cdot 2H_2O$; (viii) $Cu^{II}Br_2$, under refluxing condition

150(2) K for **1**(**a** and **b**) **2**, **3**, **4**, and **7** and at 120(2) K for **9** and **12** using graphite-monochromated Mo−Kα radiation ($\lambda = 0.71073$ Å). The data were processed with SAINT,[54] and absorption corrections were made with SADABS.[54] The structures were solved by direct and Fourier methods and refined by full-matrix least-squares methods based on F^2 using SHELX-97.[55] For the structure solutions and refinements the SHELX-TL software package[56] was used. The disordered halogen positions of Cl and Br in **3**, **4**, **9**, and **12** were refined with metal−halogen and carbon−halogen distances restrained (DFIX). Due to minor site occupation the Cl(1), Cl(2), Br(3), and Br(4) positions in **3**, the Cl(3) position in **4**, and the Cl(1) position in **12** were refined isotropically. For **2,** the very low occupation factors of 0.04 to 0.08 for the Cl(1), Cl(2), Br(3) and Br(4) positions allowed no independent refinement with distinct Cl and Br positions, but positions and displacement parameters were constrained (EXYZ, EADP). Accordingly, the derived geometric parameters for **2** are less meaningful. The non-hydrogen atoms were refined anisotropically, while the hydrogen atoms from difference Fourier maps were placed at idealized positions with fixed thermal parameters. Crystal data and details of structure determinations are summarized in Table 1.

Results and Discussion

Synthesis. The synthesis of copper(I), copper(II), nickel(II), and cobalt(II) complexes, including the halogen-exchanged products 6,6′-bis(halomethyl)-2,2′-bipyridine bpy-Br_2 ($C_{12}H_{10}N_2Br_2$) and bpy-Cl_2 ($C_{12}H_{10}N_2Cl_2$), are outlined in Scheme 1. The copper(I) complex $[Cu(bpy\text{-}Br_2)_2](ClO_4)$ (**1**) has been isolated in two crystallographic modifications (**1a**, **1b**), of which, **1a** has been straightforwardly obtained by reacting $[Cu(CH_3CN)_4](ClO_4)$ with the ligand in 1:2 ratio. Alternatively, a mixture of $Cu(ClO_4)_2 \cdot 6H_2O$ (1 equiv) and bpy-Br_2 (2 equiv) in methanol−chloroform solution gradually changes color from green to yellow-green to orange-red, and upon removal of the solvent, instead of the expected product $[Cu(bpy\text{-}Br_2)_2](ClO_4)_2$, a mixture of two crystalline materials has been obtained. The major fraction, obtained as red crystals, has been identified as the second crystallographic modification of $[Cu^{I}(bpy\text{-}Br_2)_2](ClO_4)$ (**1b**), while the minor yellowish-green fraction has been analyzed to have the composition $[Cu^{II}(bpy\text{-}Br_2)(H_2O)_3](ClO_4)_2$. It appears that $[Cu^{II}(bpy\text{-}Br_2)_2]^{2+}$ is thermodynamically unstable and in solution autocatalytically reduces to $[Cu^{I}(bpy\text{-}Br_2)_2]^{+}$. Even $[Cu^{II}(bpy\text{-}Br_2)(H_2O)_3]^{2+}$ in methanol solution undergoes ligand dissociation. The autocatalytic formation of **1b** from a 1:2 mixture of $Cu(ClO_4)_2 \cdot 6H_2O$ and bpy-Br_2 in methanol-chloroform medium has been followed spectrophotometrically (Figure 1). It may be noted that with the passage of time a new band is developed at 450 nm due to the LMCT transition of **1b**, which grows in intensity as the concentration of the reduced complex (**1b**) increases. In contrast, the intensity of the relatively weak and broad d−d band of copper(II) at 750 nm decreases with time.

The reaction between $CuCl_2 \cdot 2H_2O$ and bpy-Br_2 in equimolar ratio leads to the formation of several complexes in which the chlorine and bromine atoms are exchanged between the ligand and metal sites to different extents. The extent of redistribution of the halogens depends upon time and temperature of reaction. Thus, the product isolated soon after reacting $CuCl_2 \cdot 2H_2O$ with bpy-Br_2 and $CuBr_2$ with bpy-Cl_2 in methanol−chloroform at room temperature have the compositions $[Cu^{II}(bpy\text{-}Br_2)Cl_2]$ (**5**) and $[Cu^{II}(bpy\text{-}Cl_2)Br_2]$ (**6**), showing that no exchange have taken place under this condition. However, by extending the reaction time or by increasing the reaction temperature the following products have been isolated: $[Cu^{II}(bpy\text{-}Br_{1.86}Cl_{0.14})(Cl_{1.89}Br_{0.11})]$ (**2**), $[Cu^{II}(bpy\text{-}Br_{1.81}Cl_{0.19})(Cl_{1.70}Br_{0.30})(H_2O)]$ (**3**), and $[Cu^{II}(bpy\text{-}Br_{0.63}Cl_{1.37})(Cl_{0.54}Br_{1.46})]$ (**4**). The color of $[Cu^{II}(bpy\text{-}Br_{2-x}Cl_x)(Cl_{2-y}Br_y)]$ compounds depend upon the values of x and y and they change in the order: red (**2**) → green (**3**) → maroon (**4**). Again, $[Cu^{II}(bpy\text{-}Br_2)Cl_2]$ (**5**) is light red, $[Cu^{II}(bpy\text{-}Cl_2)Br_2]$ (**6**) is dark brown, and $[Cu^{II}(bpy\text{-}Cl_2)Cl_2]$ (**7**) is orange-red, whereas $[Cu^{II}(bpy\text{-}Cl_2)(H_2O)Cl_2]$ (**8**), similar to compound **3**, is green.

In sharp contrast to the formation of $[Cu^{II}(bpy\text{-}Cl_2)Br_2]$ (**6**) at room temperature, if the reaction between bpy-Cl_2 and

(54) SAINT (version 6.02), SADABS (version 2.03), Bruker AXS lnc., Madison, Wisconsin, 2002.
(55) Sheldrick, G. M.; SHELXL-97, *Program* for the Refinement of crystal Structures, University of Göttingen, Göttingen, Germany, 1997.
(56) SHELXTL (version 6.10), Bruker AXS Inc., Madison, Wisconsin, 2002.

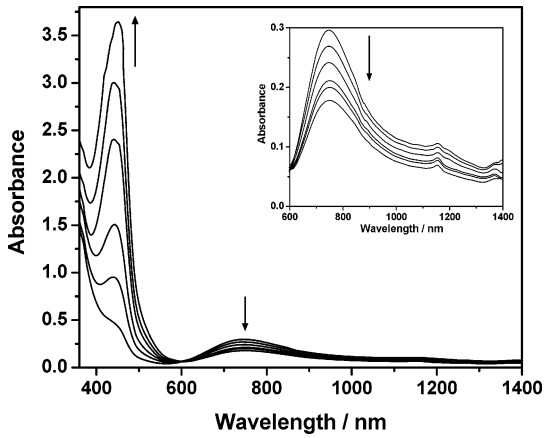

Figure 1. Spectral changes recorded at various time intervals for a 1:2 mixture of $Cu(ClO_4)_2 \cdot 6H_2O$ and bpy-Br_2 in methanol−chloroform (5×10^{-3} M) at room temperature.

$CuBr_2$ is carried out under refluxing condition, the reduction of the metal center as well as halogen exchange and scrambling at the ligand site take place. The product isolated is a brown dimeric copper(I) complex of composition $[\{Cu^{I}(bpy\text{-}Cl_{1.30}Br_{0.70})(\mu\text{-}Br)\}_2]$ (**9**). Similarly, the reaction between bpy-Br_2 and $CuBr_2$ under refluxing condition has led to the isolation of $[\{Cu^{I}(bpy\text{-}Br_2)(\mu\text{-}Br)\}_2]$ (**10**). Finally, the halogen-exchanged compounds $[Co^{II}(bpy\text{-}Br_{0.5}Cl_{1.5})(ClBr)]$ (**11**) and $[Ni^{II}(bpy\text{-}Br_{0.46}Cl_{1.54})(H_2O)(Cl_{0.73}Br_{1.27})]$ (**12**) have been obtained by reacting bpy-Br_2 with the corresponding hydrated metal chlorides under boiling condition.

It may be noted that the halide-exchanged modified ligands bpy-$Br_{2-x}Cl_x$ thus formed can be easily isolated by demetallating the metal complexes. For example, the copper(II) complexes can be demetalated by treating with sodium hydrosulfide, while the nickel(II) complex readily liberates the ligand when it is boiled with methanol in the presence of sulfuric acid as a catalyst.

Characterization. The characterization data for all of the compounds are given in Experimental Section. The ESI−MS of the copper(II) complexes **2**−**5** have been examined with their acetonitrile solutions. However, the spectral features exhibited by all the four compounds turned out to be similar. The observed and simulated isotopic distribution patterns of $[Cu^{II}(bpy\text{-}Br_2)Cl_2]$ (**5**), which is typical of the series, is shown in Figure S1 of the Supporting Information. The positively charged species detected include, $[Cu(bpy\text{-}Br_2)_2]^+$ (m/z = 746.34), $[Cu(bpy\text{-}Br_2)(bpy\text{-}Br)]^+$ (m/z = 668.47), $[Cu(bpy\text{-}Br_2)]^+$ (m/z = 404.61), $[Cu(bpy\text{-}BrCl)]^+$ (m/z = 360.69), $[Cu(bpy\text{-}Br)]^+$ (m/z = 326.75), and $[Cu(bpy\text{-}Cl)]^+$ (m/z = 280.64). It may be noted that under the conditions used for ionization, reduction of copper(II) to copper(I), exchange of the halogen atoms, and fragmentation of the ligand unit took place. The mass spectra observed for the two forms of $[Cu^{I}(bpy\text{-}Br_2)_2](ClO_4)$ (**1a**/**1b**) are identical and they exhibit two peaks due to $[Cu^{I}(bpy\text{-}Br_2)_2]^+$ (15%; m/z = 746.34) and $[Cu^{I}(bpy\text{-}Br_2)]^+$ (100%; m/z = 404.61).

The proton NMR spectra of the copper(I) complexes $[Cu^{I}(bpy\text{-}Br_2)](ClO_4)$ (**1**), $[\{Cu^{I}(bpy\text{-}Cl_{1.30}Br_{0.70})(\mu\text{-}Br)\}_2]$ (**9**), and $[\{Cu^{I}(bpy\text{-}Br_2)(\mu\text{-}Br)\}_2]$ (**10**) (Figure S2 of the Supporting Information) show only small differences in chemical shifts

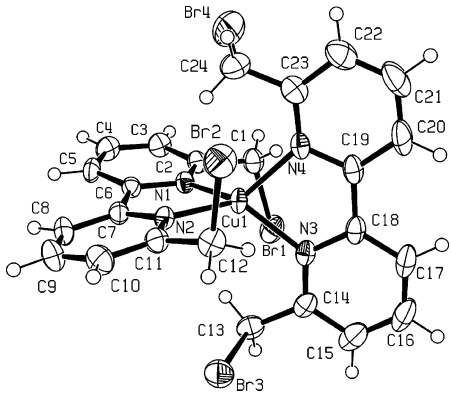

Figure 2. ORTEP representation of the cation of one of the polymorph of $[Cu^{I}(bpy\text{-}Br_2)_2](ClO_4)$ (**1a**) showing 50% probability displacement ellipsoids.

Table 2. Selected Bond Distances (Å) and Angles (deg) for Complexes **1a** and **1b**

1a		**1b**	
Cu(1)−N(1)	2.025(3)	Cu(1)−N(11)	2.021(5)
Cu(1)−N(2)	2.028(3)	Cu(1)−N(12)	2.014(5)
Cu(1)−N(3)	2.025(3)	Cu(1)−N(13)	2.016(5)
Cu(1)−N(4)	2.026(3)	Cu(1)−N(14)	2.020(5)
		Cu(2)−N(21)	2.009(5)
		Cu(2)−N(22)	2.030(5)
		Cu(2)−N(23)	2.016(5)
		Cu(2)−N(24)	2.019(5)
N(1)−Cu(1)−N(3)	127.75(10)	N(12)−Cu(1)−N(13)	124.5(2)
N(1)−Cu(1)−N(4)	123.34(11)	N(12)−Cu(1)−N(14)	123.3(2)
N(3)−Cu(1)−N(4)	81.36(11)	N(13)−Cu(1)−N(14)	81.4(2)
N(1)−Cu(1)−N(2)	81.22(10)	N(12)-Cu(1)−N(11)	81.4(2)
N(3)−Cu(1)−N(2)	124.77(11)	N(13)−Cu(1)−N(11)	130.8(2)
N(4)−Cu(1)−N(2)	124.71(10)	N(14)−Cu(1)−N(11)	121.6(2)
		N(21)−Cu(2)−N(23)	128.65(19)
		N(21)−Cu(2)−N(24)	120.30(19)
		N(23)−Cu(2)−N(24)	81.1(2)
		N(21)−Cu(2)−N(22)	80.7(2)
		N(23)−Cu(2)−N(22)	128.2(2)
		N(24)−Cu(2)−N(22)	124.0(2)

due to the pyridine ring protons. Thus, while for **1**, the doublet due to H(5), the triplet due to H(4), and the doublet due to H(3) are observed at 8.42, 8.16, and 7.76 ppm, respectively, for both **9** and **10**, these resonances occur at 8.40, 8.11, and 7.80 ppm. In contrast, the chemical shifts due to the methylene protons for the three compounds, 4.39 (**1**), 4.70 (**9**), and 4.53 (**10**) ppm, differ substantially.

The characterization data for the modified ligands bpy-$Br_{2-x}Cl_x$, have been compared with those of bpy-Br_2 and bpy-Cl_2 in the Experimental Section. As may be noted, the ESI−MS for bpy-$Br_{1.81}Cl_{0.19}$, bpy-$Br_{0.63}Cl_{1.37}$, and bpy-$Br_{0.46}Cl_{1.54}$ do not provide peaks due to their molecular ion. Alternatively, in all of the cases, singly charged positive ions due to (bpy-Br_2 + Na^+), (bpy-Br_2 + H^+), (bpy-BrCl + Na^+), (bpy-BrCl + H^+), (bpy-Br + H^+), (bpy-Cl_2 + Na^+), (bpy-Cl_2 + H^+), and (bpy-Cl + H^+) have been observed, albeit with differing intensity ratios.

The ^{1}H NMR spectral patterns for the aromatic protons of bpy-Br_2 and bpy-Cl_2 are practically identical. However, the protons due to CH_2−Br and CH_2−Cl occur at 4.68 and 4.75 ppm, respectively. As given in the Experimental Section, for all of the bpy-$Br_{2-x}Cl_x$ compounds, both of the singlets are observed at their expected positions, but with differing peak areas. The ratio of these two peaks are in agreement

Table 3. Selected Bond Distances (Å) and Angles (deg) for Complexes **2**, **3**, **4**, and **7**[a]

2		**3**		**4**		**7**	
Cu(1)−N(1)	1.990(5)	Cu(1)−O(1)	1.958(2)	Cu(1)−N(1)	2.011(3)	Cu(1)−N(1)	2.015(4)
Cu(1)−N(2)	2.007(6)	Cu(1)−N(1)	2.209(2)	Cu(1)−N(2)	2.021(3)	Cu(1)−N(2)	2.005(4)
Cu(1)−Cl(3)	2.233(2)	Cu(1)−N(2)	1.999(2)	Cu(1)−Br(3)	2.3379(8)	Cu(1)−Cl(3)	2.2279(1 4)
Cu(1)−Cl(4)	2.210(2)	Cu(1)−Cl(3)	2.301(3)	Cu(1)−Br(4)	2.342(3)	Cu(1)−Cl(4)	2.2079(1 5)
Br(1)−C(1)	1.942(7)	Cu(1)−Cl(4)	2.315(3)	Cl(1)−C(1)	1.786(7)	Cl(1)−C(1)	1.783(5)
Br(2)−C(12)	1.893(7)	Br(1)−C(1)	1.944(3)	Cl(2)−C(12)	1.790(7)	Cl (2)−C(12)	1.783(5)
		Br(2)−C(12)	1.950(3)				
N(1)−Cu(1)−N(2)	82.4(2)	O(1)−Cu(1)−N(1)	104.25(9)	N(1)−Cu(1)−N (2)	82.42(12)	N(1)−Cu(1)−N(2)	82.19(16)
N(1)−Cu(1)−Cl(3)	106.31(17)	O(1)−Cu(1)−N(2)	174.28(9)	N(1)−Cu(1)− Br(3)	135.79(9)	N(1)−Cu(1)− Cl(3)	105.12(1 0)
N(1)−Cu(1)−Cl(4)	133.29(17)	O(1)−Cu(1)−C l(3)	87.15(1 7)	N(1)−Cu(1)− Br(4)	106.35(1 8)	N(1)−Cu(1)− Cl(4)	138.05(1 2)
N(2)−Cu(1)−Cl(3)	123.95(16)	O(1)−Cu(1)−C l(4)	89.54(1 1)	N(2)−Cu(1)− Br(3)	102.02(9)	N(2)−Cu(1)− Cl(3)	127.45(1 2)
N(2)−Cu(1)−Cl(4)	101.42(17)	N(1)−Cu(1)−N(2)	79.30(8)	N(2)−Cu(1)−Br(4)	126.1(2)	N(2)−Cu(1)− Cl(4)	101.69(1 2)
Cl(3)−Cu(1)−Cl(4)	109.20(7)	N(1)−Cu(1)−C l(3)	99.55(1 5)	Br(3)−Cu(1)− Br(4)	105.79(1 7)	Cl(3)−Cu(1)− Cl(4)	104.92(5)
		N(1)−Cu(1)−C l(4)	101.48(11)				
		N(2)−Cu(1)−C l(3)	87.82(1 7)				
		N(2)−Cu(1)−C l(4)	94.17(1 1)				
		Cl(3)−Cu(1)−Cl(4)	158.68(16)				

[a] Only major positions of disordered halogen atoms are listed.

Table 4. Selected Bond Distances (Å) and Angles (deg) for Complex **9**[a]

9			
Cu(1)−N(1)	2.075(7)	Cu(1)#1−Br(1)−Cu(1)	84.25(5)
Cu(1)−N(2)	2.077(8)	N(1)−Cu(1)−N(2)	80.2(3)
Cu(1)−Br(1)	2.4670(15)	N(1)−Cu(1)−Br(1)	119.8(2)
Cu(1)#1−Br(1)	2.4503(15)	N(1)−Cu(1)−Br(1)#1	127.2(2)
Cu(1)−Br(1) #1	2.4503(15)	N(2)−Cu(1)−Br(1)	118.5(2)
Cl(2)−C(1)	1.919(15)	N(2)−Cu(1)−Br(1)#1	117.4(2)
Cl(3)−C(12)	1.882(18)	Br(1)#1−Cu(1)−Br(1)	95.75(5)
			84.25(5)

[a] Only major positions of disordered halogen atoms are listed.

Table 5. Selected Bond Distances (Å) and Angles (deg) for Complex **12**[a]

12			
Ni(1)−O(1)	1.998(2)	Ni(1)−Br(1)	2.4502(7)
Ni(1)−N(1)	2.027(2)	Ni(1)−Br(2)	2.481(13)
Ni(1)−N(2)	2.033(3)	Cl(3)−C(1)	1.842(9)
		Cl(4)−C(12)	1.819(6)
O(1)−Ni(1)−N(1)	164.17(11)	N(1)−Ni(1)−Br(1)	93.48(7)
O(1)−Ni(1)−N(2)	113.20(11)	N(1)−Ni(1)−Br(2)	87.9(2)
O(1)−Ni(1)−Br(1)	88.34(7)	N(2)−Ni(1)−Br(1)	102.46(7)
O(1)−Ni(1)−Br(2)	86.0(2)	N(2)−Ni(1)−Br(2)	94.0(2)
N(1)−Ni(1)−N(2)	81.78(11)	Br(1)−Ni(1)−Br(2)	163.5(2)

[a] Only major positions of disordered halogen atoms are listed.

with their expected compositions. It may be noted that unlike bpy-Br_2 and bpy-Cl_2, aromatic protons of bpy-$Br_{2-x}Cl_x$ compounds are expectedly observed as multiplets rather than as doublet, triplet, and doublet.

Crystal Structures. The X-ray crystal structures of complexes **1a**, **1b**, **2**, **3**, **4**, **7**, **9**, and **12** have been determined, and their relevant bond distances and angles are given in Table 2−5.

$[Cu^I(bpy\text{-}Br_2)](ClO_4)$ (1a, 1b). The copper(I) complex $[Cu^I(bpy\text{-}Br_2)](ClO_4)$ (**1**) has been obtained in two crystallographic modifications **1a** and **1b**, which differ in their unit cell dimensions and space groups. The space group of **1a** is $P2_1/n$ and it has 1 molecule per asymmetric unit, whereas the space group of **1b** is $P2_1/c$ and it contains 2 independent molecules per asymmetric unit. The ORTEP representations of the cations in **1a** and **1b** (for one of the two identical structures) are shown in Figures 2 and S3 (see the Supporting Information), whereas their bond distances and angles are compared in Table 2. As may be noted, the Cu−N distances in **1a** (2.026(2) Å) are more uniform relative to those of **1b**, which lie in the range from 2.009(5) to 2.030(5) Å. The dihedral angles (θ) between the two CuN_2 planes are 87.9(1)° in **1a**, and 86.4(1)° and 87.8(1)° in the two complex units of **1b**. The near orthogonality of the two bpy-Br_2 ligands in the complex cations indicate almost ideal tetrahedral D_{2d} geometry for the copper(I) center. By comparison, the values of θ in $[Cu(Me_2\text{-}bpy)_2](ClO_4)$ and $[Cu(bpy)_2](ClO_4)$ are 80.64°[35b,57] and 75.2°,[58] respectively. The greater steric interaction exerted by the bulkier CH_2Br substituents in bpy-Br_2 relative to the methyl substituents in 6,6′-Me_2bpy in their corresponding copper(I) complexes is clearly evident. Aside from the small differences in the θ values of **1a** and **1b**, they also show some difference in the twist angles between then pyridine ring planes about 2,2′ C−C bond, which are 13.5° and 2.4° in **1a**, 14.7° and 9.5° in molecule 1 of **1b**, and 17.1° and 5.8° in molecule 2 of **1b**.

There is considerable structural difference between **1a** and **1b** in terms of intermolecular C−H···O hydrogen bonding. As shown in Figure S4(a) of the Supporting Information, the pyridyl hydrogens attached to C(17) and C(20) in **1a** are hydrogen bonded to the oxygen atoms O(11) and O(14), respectively of the perchlorate anion belonging to the adjacent complex molecule. The C(17)−H···O(11) and C(20)−H···O(14) distances are 2.45 and 2.36 Å, respectively, and the corresponding bond angles are 143.8° and 149.4°. Similar C−H···O bonding is absent in either of the two molecules in **1b**. Alternatively, as shown in Figure S4(b) of the Supporting Information, a different type of bifurcated C−H···O bonding is observed in **1b** involving a perchlorate oxygen and one each CH_2Br hydrogen atoms of the two complex cations of **1b**.

$[Cu^{II}(bpy\text{-}Br_{1.86}Cl_{0.14})(Cl_{1.89}Br_{0.11})]$ (2), $[Cu^{II}(bpy\text{-}Br_{1.81}Cl_{0.19})(Cl_{1.70}Br_{0.30})(H_2O)]$ (3), $[Cu^{II}(bpy\text{-}Br_{0.63}Cl_{1.37})(Cl_{0.54}Br_{1.46})]$ (4), and $[Cu^{II}(bpy\text{-}Cl_2)Cl_2]$ (7). As already stated, the reaction between the ligand bpy-Br_2 and $CuCl_2$·

(57) Burke, P. J.; McMillin, D. R.; Robinson, W. R. *Inorg. Chem.* **1980**, *19*, 1211.
(58) Munakata, M.; Kitagawa, S.; Asahara, A.; Masuda, H. *Bull. Chem. Soc. Jpn.* **1987**, *60*, 1927.

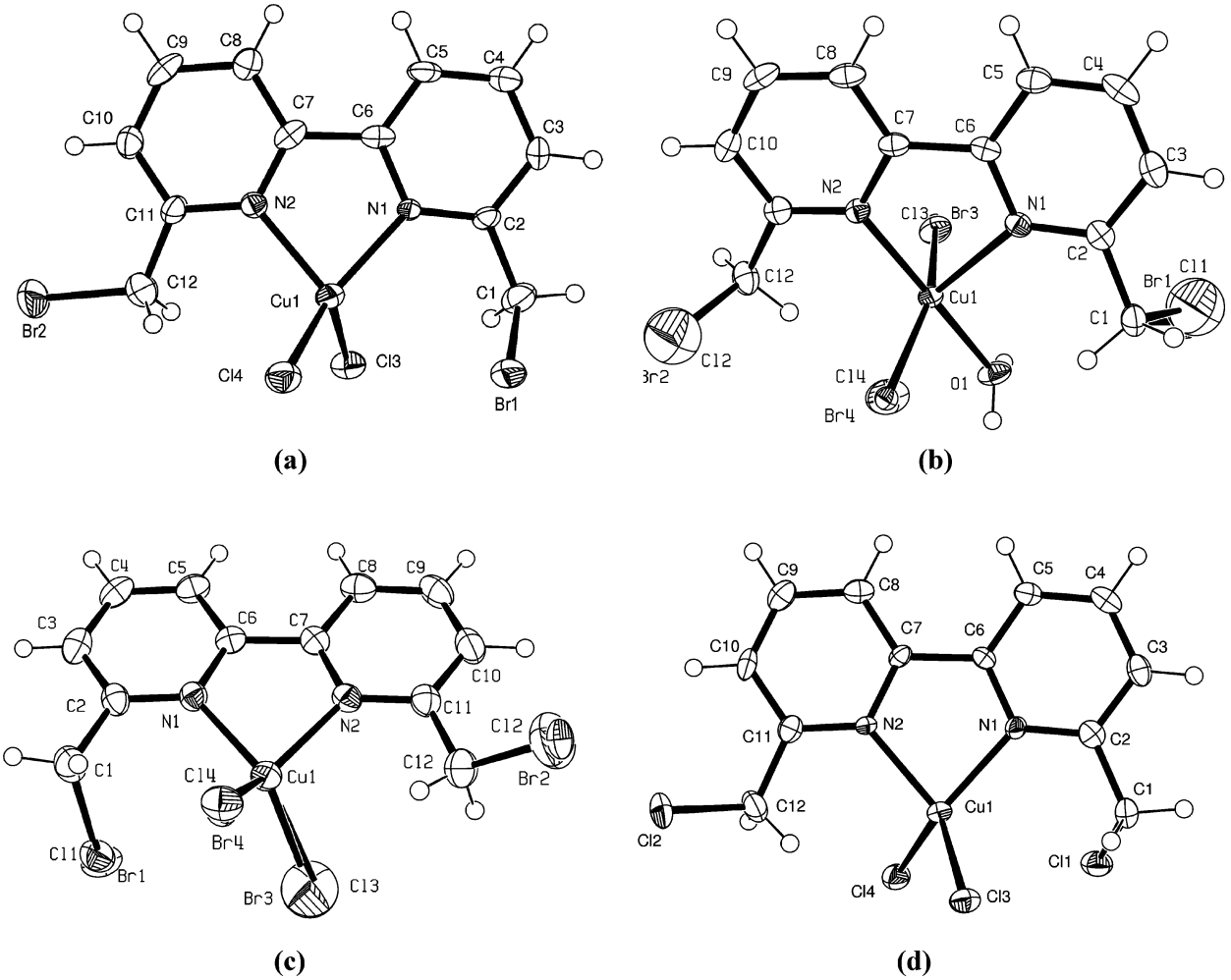

Figure 3. ORTEP representations of (a) $[Cu^{II}(bpy\text{-}Br_{1.86}Cl_{0.14})(Cl_{1.89}Br_{0.11})]$ (**2**), only major halogen position shown, (b) $[Cu^{II}(bpy\text{-}Br_{1.81}Cl_{0.19})(Cl_{1.70}Br_{0.30})(H_2O)]$ (**3**), and (c) $[Cu^{II}(bpy\text{-}Br_{0.63}Cl_{1.37})(Cl_{0.54}Br_{1.46})]$ (**4**) and (d) $[Cu^{II}(bpy\text{-}Cl_2)Cl_2]$ (**7**) showing 50% probability displacement ellipsoids.

$2H_2O$ leads to the formation of copper(II) complex [Cu(bpy-Br_2)Cl_2], provided the reaction time is short. If the reaction mixture is kept for a longer period or is heated under reflux, then halogen exchange takes place between bpy-Br_2 and $CuCl_2$ and the composition of the product isolated depends upon the reaction condition. The ORTEP representations of **2**−**4** and of $[Cu^{II}(bpy\text{-}Cl_2)Cl_2]$ (**7**) are shown in Figure 3, parts a−d, although for compound **2** only the major position of disordered halogen atoms are shown.

Compounds **2** and **4** are tetracoordinated, whereas **3** is pentacoordinated. According to the disorder of halogen positions (see above), compound **2** is formulated as $[Cu^{I}$-$_{I}(bpy\text{-}Br_{1.86}Cl_{0.14})(Cl_{1.89}Br_{0.11})]$, composition of **3** is $[Cu^{II}(bpy\text{-}Br_{1.81}Cl_{0.19})(Cl_{1.70}Br_{0.30})(H_2O)]$ with site occupation factors Br/Cl(1) 0.917(4)/0.083(4), Br/Cl(2) 0.894(4)/0.106(4), Br/Cl(3) 0.103(2)/0.897(2), Br/Cl(4) 0.200(3)/0.800(3), and that of compound **4** is considered to be $[Cu^{II}(bpy\text{-}Br_{0.63}Cl_{1.37})(Cl_{0.54}$-$Br_{1.46})]$ with Br/Cl(1) 0.276(3)/0.724(3), Br/Cl(2) 0.351(4)/0.649(4), Br/Cl(3) 0.840(7)/0.160(7), Br/Cl(4) 0.625(3)/0.375(3). The relevant bond distances and angles of compounds **2**−**4** are listed in Table 3.

The 4-coordinated copper(II) centers in **2** and **4** (Figures 3, parts a and c) have flattened tetrahedral geometry, as evident from the fact that in **2** and **4** the dihedral angles between the CuN_2 and $CuCl_2$ or Cu(halogen)$_2$ planes are 69.52(2)° and 67.38(3)°, respectively. The Cu−N distances in the two compounds, 1.989(5) and 2.007(6) Å in **2** and 2.012(3) and 2.020(3) Å in **4**, are comparable.

In the 5-coordinated copper(II) complex $[Cu^{II}(bpy\text{-}Br_{1.81}$-$Cl_{0.19})(Cl_{1.70}Br_{0.30})(H_2O)]$ (**3**), the metal center adopts a distorted square pyramidal geometry (Figure 3b) with the atoms N(2)Cl(1)O(1)Cl(2) forming the basal plane, while the pyridyl nitrogen N(1) is occupying the apical position. In the basal mean plane, the constituent atoms are alternatively displaced in opposite direction by 0.18 Å, albeit the metal center rests on the plane. The equatorial Cu−N(2) distance (1.999(2) Å) is considerably shorter than the apical Cu−N(1) distance (2.209(2) Å). The other equatorial bond distances are Cu−Cl(3)/ Br(3) = 2.301(3)/2.398(9) Å, Cu−Cl(4)/Br(4) = 2.315(3)/2.360(4) Å, and Cu−O(H_2O) = 1.958(2) Å. The extent of distortion from ideal square pyramidal geometry is given by the parameter τ,[59] which is 0.25 for **3** (τ = 0 and 1 are for perfectly square pyramidal and trigonal bipyramidal geometries, respectively). The two

(59) Addison, A. W.; Rao, T. N.; Reedijk, J.; van Rijn, J.; Vershoor, G. C.; *J. Chem. Soc., Dalton Trans.*. **1984**, 1349.

hydrogen atoms of the coordinated water molecule in compound **3** are intermolecularly hydrogen bonded with one of the metal-coordianted halogene atoms of two different complex molecules. The other metal-coordinated halogene atom, in turn, is hydrogen bonded with the coordinated water of another molecule. In this way, as shown in Figure S5 of the Supporting Information, a double helical one-dimensional network is developed in which the Cl(3)···H(2) and Cl(4)···H(1) distances are 2.249 and 2.429 Å, respectively, while the O−H···Cl angles are 166° and 160°.

As shown in Figure 3d, the structure of $[Cu^{II}(bpy\text{-}Cl_2)Cl_2]$ (**7**) is similar to those of **2** and **4**. The selected bond parameters of **7** are compared with those of **2** and **4** in Table 3. It may be noted that the Cu−N distances and N−Cu−N angles of these three isostructural compounds are closely similar. Alternatively, the average Cu−halogen and C−halogen distances tend to increase with the replacement of chlorine by bromine. A comparison of the dihedral angle θ between CuN_2 and Cu(halide)$_2$ planes indicates that the tetrahedral distortion of the three compounds decrease in the following order: **2** (69.52)° > **4** (67.38)° > **7** (65.34)°.

$[\{Cu^{I}(bpy\text{-}Cl_{1.30}Br_{0.70})(\mu\text{-}Br)\}_2]$(9) and **$[\{Cu^{I}(bpy\text{-}Br_2)(\mu\text{-}Br)\}_2]$ (10).** When $CuBr_2$ is reacted with bpy-Cl_2 and bpy-Br_2 under refluxing condition, reduction of the metal center takes place and crystals of **9** and **10** separate out from their reaction solutions. In the case of **9**, the halogen atoms at the ligand sites are heavily disordered, although there is no disordering of the metal-coordinated bromide ligands. The resulting site occupation factors are Br/Cl(2) 0.417(8)/0.583(8) and Br/ Cl(3) 0.284(9)/0.716(9). Figure 4, parts a and b, shows the molecular structures of **9** and **10.** It should be noted that due to poor crystal quality of **10** and hence of not fully satisfying refinement we only present the structure without detailed discussion. The pertinent bond distances and bond angles for **9** are listed in Table 4. In both of the compounds, the copper(I) centers have near perfect tetrahedral geometry, as evident from the dihedral angle θ between the CuN_2 and $CuBr_2$ planes [$\theta = 87.7(3)$ for **9**]. In compound **9**, the bridge angle Cu−Br−Cu is 84.25(5)°, while the angle Br−Cu−Br is 95.75(5)°. The average Cu^{I}−N distance in **9** (2.076(8) Å), as should be expected, is longer compared to the average Cu^{II}−N distance (2.008(8) Å) observed in **2**, **4**, and **7**. The nonbonded Cu····Cu distance in **9** is 3.30 Å.

$[Ni^{II}(bpy\text{-}Br_{0.46}Cl_{1.54})(Cl_{0.73}Br_{1.27})(H_2O)]$ (12). This compound has been obtained by reacting bpy-Br_2 with $NiCl_2\cdot 6H_2O$ under refluxing condition. The halogen exchange and scrambling is quite extensive in **12**, and the halogen sites have the following occupancies: Br/Cl(1) 0.833(2)/0.167(2), Br/Cl(2) 0.439(3)/ 0.561(3), Br/Cl(3) 0.232(4)/0.768(4), Br/Cl(4) 0.226(6)/0.774(6). It is to be noted that the two bromine atoms of bpy-Br_2 are rather more uniformly substituted by chlorines, while the two chlorine atoms of $NiCl_2$ are unevenly substituted by bromines. The ORTEP representation of **12** is shown in Figure 5a, and the selected bond distances and angles are given in Table 5. Compound **12** is structurally similar to the five-coordinated copper(II) complex **3**, although the square pyramidal geometry of **12** is much more regular ($\tau = 0.015$) than that of **3** ($\tau = 0.25$). From the least-squares plane formed by N(1) O(1)Br/Cl(1)-Br/Cl(2), the displacement of the donor atoms do not exceed 0.04 Å, while the metal center lies exactly on the plane. The two in-plane bond distances, Ni−O(1) = 1.998(2) Å and Ni−N(1) = 2.027(2) Å, differ to a small extent. The bond distance involving the apical N(2) nitrogen from the metal center is 2.033(3) Å. As expected for a regular square pyramidal geometry, the two major angles viz. O(1)−Ni−N(1) (164.17(11)°) and Br(1)−Ni−Br(2)/Cl(1)-Ni−Cl(2) (163.5(2)/162.6(6)°) are almost equal. In this case also, similar to **3**, intermolecular hydrogen bonding involving the metal-coordinated water and halogens give rise to a double helical chain, whose space-filling model is shown in Figure 5b.

Absorption Spectra and Reactivities. The UV−vis-NIR absorption spectral data for compounds **1**−**12** are given in the Experimental Section. Figure 6 shows the spectral changes that occur when 1 equiv each of bpy-Br_2 and $CuCl_2\cdot 2H_2O$ are mixed together in acetonitrile at 45 °C. The initial spectrum, which shows a well-resolved peak at 440 nm and an unresolved band between 700 and 1300 nm, is identical to that observed for $[Cu^{II}(bpy\text{-}Br_2)Cl_2]$ (**5**). In **5**, the band observed at 440 nm ($\epsilon = 820\ M^{-1}cm^{-1}$) is most likely due to $Cl^- \rightarrow Cu^{II}$ ligand-to-metal charge transfer (LMCT) transition, while the broad feature observed is due to d−d transition. It should be mentioned that similar to **5**, the $Cl^- \rightarrow$ Cu LMCT band in $[Cu^{II}(bpy\text{-}Cl_2)Cl_2]$ (**7**) is also observed at 440 nm ($\epsilon = 750\ M^{-1}cm^{-1}$). Figure 6 shows that with the passage of time, the well-resolved peak at 440 nm slowly gets broadened and drifts to a lower wavelength along with the growth of intensity. The position of the very broad d−d band remains practically unaffected, albeit intensification of the band occurs to a small extent. Notable spectral change occurs between 500 and 700 nm, where the intensity of the successive absorption curves increases and gradually two weak shoulders develop. After 7 h, when no further spectral change occurs, three shoulders at 425 nm ($\epsilon = 850\ M^{-1}cm^{-1}$), 570 nm ($\epsilon \approx 300\ M^{-1}cm^{-1}$), and 630 nm ($\epsilon \approx 220\ M^{-1}cm^{-1}$) become evident along with the d−d band lying between 700 and 1300 nm ($\epsilon \approx 130\ M^{-1}cm^{-1}$). The final spectrum resembles that of $[Cu^{II}(bpy\text{-}Cl_2)Br_2]$ (**6**) whose spectral characteristics are as follows: 425 nm sh ($\epsilon \approx 1100\ M^{-1}cm^{-1}$), 570 nm sh ($\epsilon \approx 350\ M^{-1}cm^{-1}$), 630 nm sh ($\epsilon \approx 250\ M^{-1}cm^{-1}$), 880 nm ($\epsilon = 125\ M^{-1}cm^{-1}$), and 1080 nm ($\epsilon = 100\ M^{-1}cm^{-1}$). Significantly, the spectra observed for $[Cu^{II}(bpy\text{-}Br_{1.86}Cl_{0.14})(Cl_{1.89}Br_{0.11})]$ (2) and $[Cu^{II}(bpy\text{-}Br_{0.63}Cl_{1.37})(Cl_{0.54}Br_{1.46})]$ (**4**) are similar to the time interval spectra recorded after 0.5 and 3.5 h, respectively. The smooth spectral changes that are observed in Figure 6 suggest that the halogen exchange and scrambling (shown in eq 1) take place concurrently

$$bpy - Br_2 + CuCl_2 \rightarrow [Cu^{II}(bpy - Br_{2-x}Cl_x)(Cl_{2-y}Br_y)] \quad (1)$$

An important consequence of halide exchange and scrambling is manifestation of color changes in the solid state across the series. Thus, $[Cu^{II}(bpy\text{-}Br_2)Cl_2]$ (**5**) is light red,

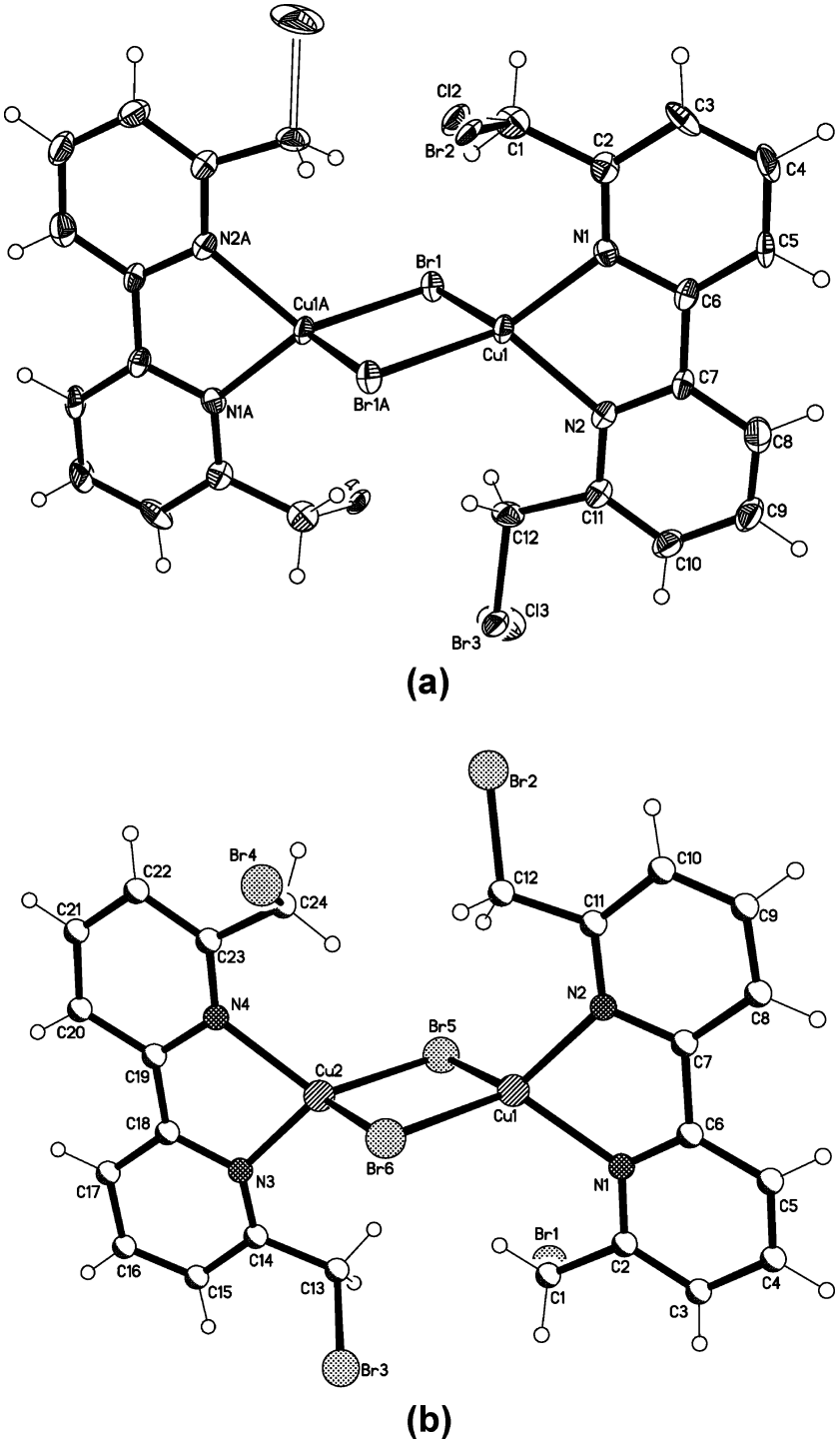

Figure 4. (a) ORTEP representations of [{Cu^{I}(bpy-$Cl_{1.30}Br_{0.70}$)(μ-Br)}$_2$] (**9**), showing 50% probability displacement ellipsoids and (b) ball and stick representation of [{Cu^{I}(bpy-Br_2)(μ-Br)}$_2$] (**10**).

[Cu^{II}(bpy-$Br_{1.86}Cl_{0.14}$)($Cl_{1.89}Br_{0.11}$)] (**2**) is red, [Cu^{II}(bpy-$Br_{1.81}$-$Cl_{0.19}$)($Cl_{1.70}Br_{0.30}$)(H_2O)] (**3**) is green, [Cu^{II}(bpy-$Br_{0.63}$-$Cl_{1.37}$)($Cl_{0.54}Br_{1.46}$)] (**4**) is maroon, and [Cu(bpy-Cl_2)Br_2] (**6**) is dark brown. Among these compounds, except for **3**, all others are 4-coordinate with flattened tetrahedral geometry. Therefore, the difference of color among the pseudo-tetrahedral compounds seems to be related with the relative contributions of $Cl^-\rightarrow Cu^{II}$ and $Br^-\rightarrow Cu^{II}$ LMCT transition energies. A comparison of the spectral features of the two terminal members [Cu^{II}(bpy-Br_2)Cl_2] (**5**) and [Cu^{II}(bpy-Cl_2)-Br_2] (**6**) reveals that in the UV-region both the compounds exhibit two bands at about 250 and 310 nm due to $\pi-\pi^*$ transitions of the bpy ligands. However, while for **5** a $Cl^-\rightarrow Cu^{II}$ LMCT band[60] is observed at 440 nm (ϵ = 820 $M^{-1}cm^{-1}$), in the case of **6**, three LMCT bands ($Br^-\rightarrow Cu^{II}$) are observed at 425 nm ($\epsilon \approx 1100$ $M^{-1}cm^{-1}$), 570 nm ($\epsilon \approx$ 350 $M^{-1}cm^{-1}$), and 630 nm ($\epsilon \approx 250$ $M^{-1}cm^{-1}$). The occurrence of LMCT bands above 500 nm in $Cu^{II}N_2Br_2$

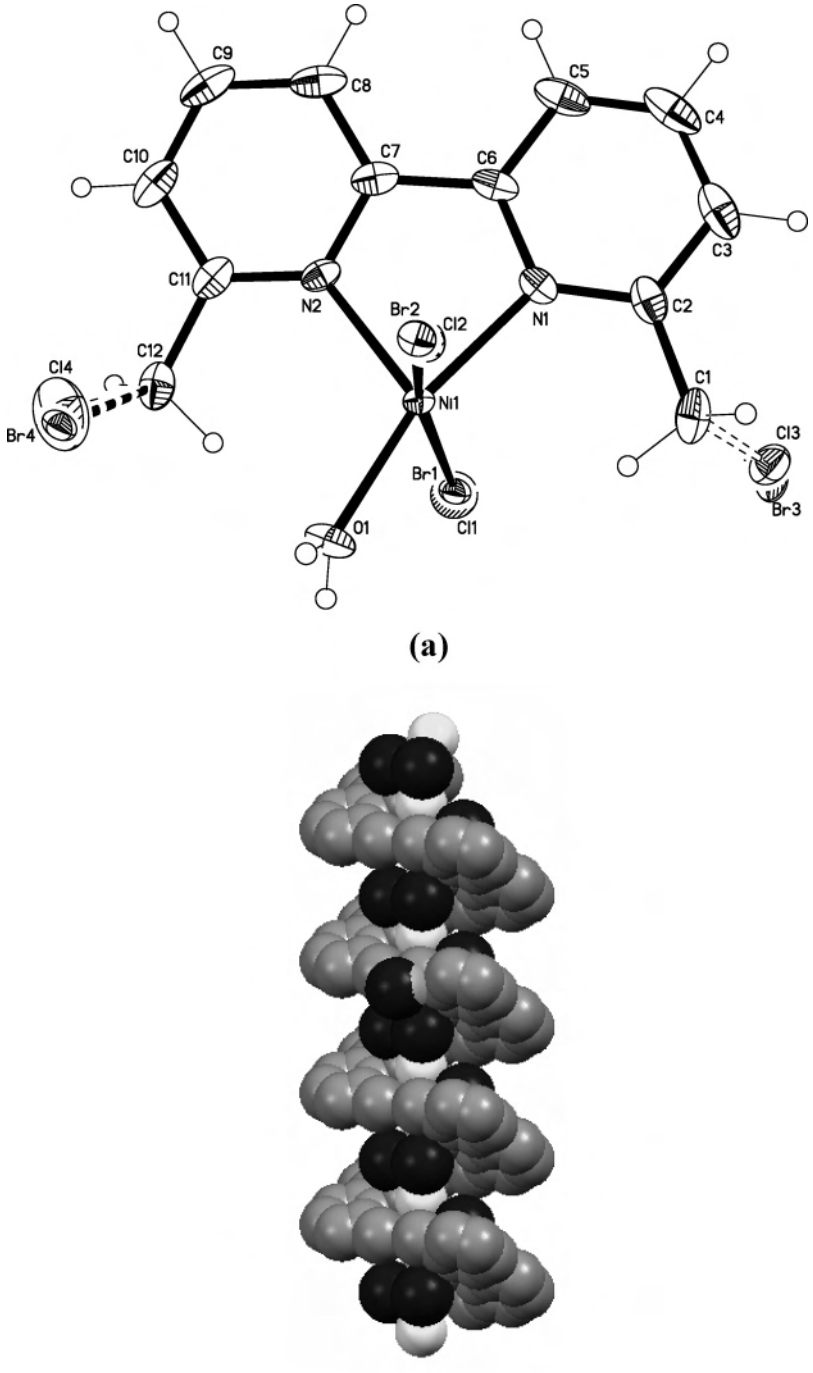

Figure 5. (a) An ORTEP view of [Ni(bpy-$Br_{0.46}Cl_{1.54}$)($Cl_{0.73}Br_{1.27}$)(H_2O)] (**12**) and (b) A space-filling representation of doubly helical one-dimensional chain formed by Cl···H−O−H···Cl hydrogen bondings in **12**.

chromophores have been reported in literature.[46,60−62] The weak intensity of $Br^- \rightarrow Cu^{II}$ LMCT band at higher wavelength has been considered to be due to forbidden or weakly allowed $2\pi p \rightarrow d\sigma^*$ transition.[63]

The structural data of the 4-coordinate copper(II) complexes **2**, **4**, and **7** (also **6**) suggest D_2 symmetry for these compounds. Alternatively, the structure of the 5-coordinate compound **3** (also **8**) indicates pseudo-C_{4v} symmetry. Although a maximum of four d−d transitions can be expected for these compounds, in all the cases a broad absorption feature covering the range from 700 to 1300 nm have been observed. This broad feature, on Gaussian analysis gets

(60) Lever, A. B. P. *Inorganic Electronic Spectroscopy*, 2nd. ed., Elsevier, Amsterdam, 1984.
(61) Solomon, E. I.; Penfield, K. W.; Wilcox, D. E. *Struct. Bonding (Barlin)*, **1983**, *53*, 1.
(62) Ray, N.; Tyagi, S.; Hatahway, B. *J. Chem. Soc., Dalton Trans*. **1982**, 143.
(63) Crutchley, R. J.; Hynes, R.; Gabe, E. J. *Inorg. Chem.* **1990**, *29*, 4921.

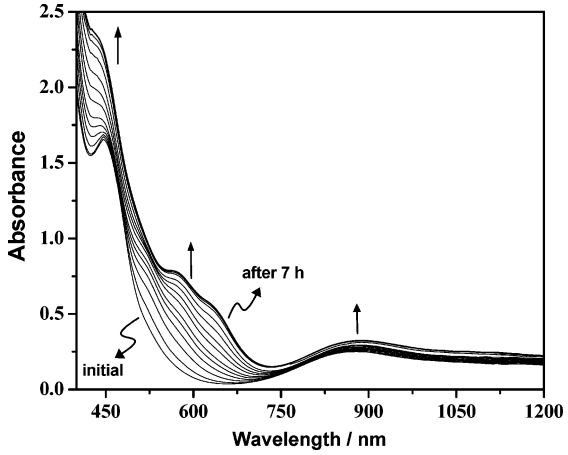

Figure 6. Spectral changes recorded at various time intervals of a 1:1 mixture of $CuCl_2 \cdot 2H_2O$ and bpy-Br_2 in acetonitrile (2.5×10^{-3} M) at 45 °C over a period of 7 h.

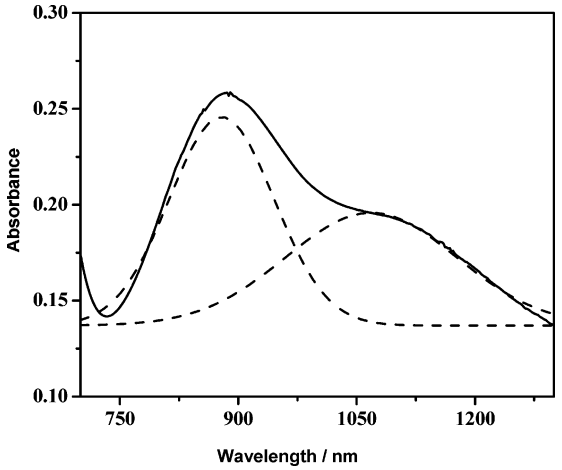

Figure 7. Observed and deconvoluted absorption spectrum of [Cu^{II}(bpy-Cl_2)Br_2)] (**6**) in the vis-NIR region obtained by Gaussian analysis.

deconvoluted to two well-defined bands with their peaks lying at about 850−880 nm and 970−1090 nm. A typical deconvoluted spectrum obtained for compound **6** is shown in Figure 7, for which the two peaks are located at 880 and 1080 nm.

It would be relevant at this stage to consider the mechanism of halogen exchange and scrambling in the light of the molecular structures determined for the copper(II) complexes **2**−**4** and the nickel(II) complex **12**. The noteworthy aspect of these compounds is that the distribution of the halogen atoms is not the same either in the 6- and 6′-halomethyl moieties of the ligands or in the two metal coordinated halides. To account for this observation, an intramolecular atom transfer reaction that occurs in a randomized way is outlined in Scheme 2.

The reactivities of copper(II) bromide with bpy-Cl_2 and bpy-Br_2 are of particular interest. When a 1:1 mixture of bpy-Cl_2 and $CuBr_2$ in methanol−chloroform is allowed to react at room temperature for a short period, the product isolated has the composition [Cu^{II}(bpy-Cl_2)Br_2] (**6**). However, when this reaction is carried out at the boiling temperature of the solvent the product isolated (in 40% yield) has the

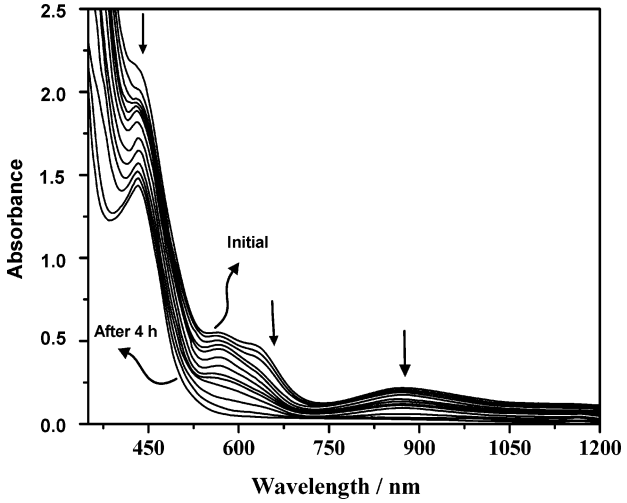

Figure 8. Spectral changes recorded after quench cooling at different time intervals of a boiling solution of [Cu^{II}(bpy-Cl_2)Br_2)] (**6**) in acetonitrile (2.5×10^{-3} M) over 4 h.

Scheme 2

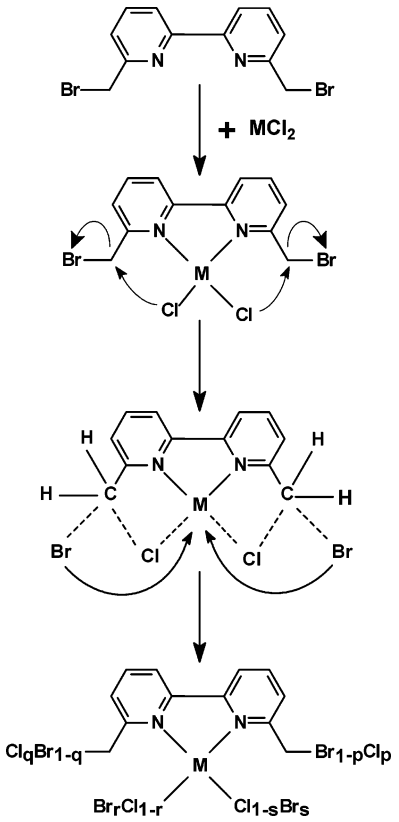

composition [{Cu^{I}(bpy-$Cl_{1.30}Br_{0.70}$)(μ-Br_2)}$_2$] (**9**). Again, under the boiling condition, the reaction between bpy-Br_2 and $CuBr_2$ affords [{Cu^{I}(bpy-Br_2)(μ-Br_2)}$_2$] (**10**) in high yield (>80%). Further, studies have indicated that the formation of **9** and **10** actually take place through photoinduced reduction. This was borne out by the fact that a solution containing bpy-Br_2 and $CuBr_2$, upon being kept at 50 °C in darkness, shows no change in intensity of the d−d absorption band between 700 and 1300 nm over a period of 3 h. However, the same solution on being kept exposed to light

Scheme 3

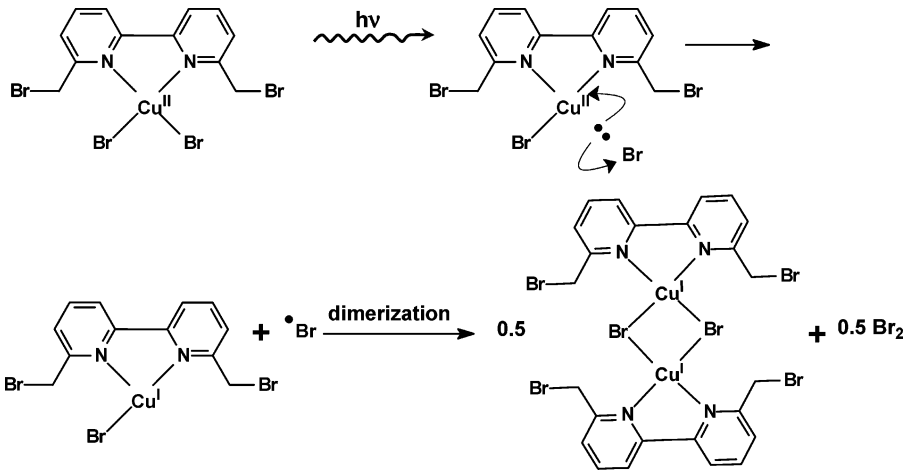

Table 6. Electrochemical Data of Complexes **1**−**10**

	acetonitrile		dichloromethan e	
compound	$E_{1/2}$ (V)	ΔE_p (mV)	$E_{1/2}$ (V)	ΔE_p (mV)
1	0.990	105	1.218	75
2	0.517	115	0.590	135
3	0.520	120	0.620	160
4	0.565	120	0.653	145
5	0.505	120	0.585	160
6	0.585	115	0.677	155
7	0.505	110	0.560	130
8	0.520	115	0.573	135
9	0.600	120		
10	0.610	100		

completely lose the d−d band over the same time period. The overall redox reaction (eq 2) seems to be initiated by

$$Cu^{II}Br_2 + \text{bpy-}Br_2 \rightarrow [Cu^{II}(\text{bpy-}Br_2)Br_2] \xrightarrow{h\nu} 0.5\,[\{Cu^{I}(\text{bpy-}Br_2)(\mu\text{-}Br)\}_2] + 0.5\,Br_2 \quad (2)$$

photoinduced homolytic cleavage of a Cu^{II}−Br bond, and is followed by dimerization, as illustrated in Scheme 3.

The formation of **9** appears to involve a more complex route because in this case along with photoreduction and dimerization halogen exchange also occurs. The molecular structure of **9** shows that despite extensive halogen exchange and scrambling of the 6- and 6′-chloromethyl sites of the ligand, the bridging bromides remain unexchanged. Further, **9** is isolated at a significantly lower yield relative to that of **10**. This indicates that during the formation of **9** other related copper(I) complexes also form although **9** preferentially crystallized out from the mixture of products. Nevertheless, the common structural features of **9** and **10** suggest that the key step involved in the formation of the two compounds is the same, that is photoinduced homolytic cleavage of a Cu^{II}−Br bond of their respective precursor complexes.

To follow the course of photoinduced reduction of [Cu^{II}-(bpy-Cl_2)Br_2] (**6**), Figure 8 shows the spectral changes that occurred when an acetonitrile solution of **6** (2×10^{-3} M) was heated under reflux in the presence of light and the spectra recorded at different time intervals after quench-cooling of the solution. As may be noted that with the passage of time, the intensities of the three shoulders observed for **6** at 425, 570, and 630 nm, as well as the broad d−d band observed in the range from 700 to 1300 nm, diminished gradually. After 4 h, all of these absorption features are replaced by a single peak at 440 nm. The total lack of absorbance in the vis-NIR region is a clear signature of the complete reduction of copper(II) to copper(I). When the same experiment was carried out in the dark, only small changes in intensities of the shoulders, but no changes in the intensities of the d−d band, were observed. Clearly, in the absence of light, only halogen exchange took place in **6** at the elevated temperature.

Compounds **9** and **10** exhibit metal to ligand ($Cu^{I} \rightarrow$ bpy-X_2 π^*) charge transfer (MLCT) transition at 440 nm, and their molar extinction coefficient values in acetonitrile are 2800 and 2600 M^{-1} cm^{-1}, respectively. By comparison, the MLCT band for the mononuclear copper(I) complex [Cu-(bpy-Br_2)$_2$](ClO_4) (**1**) observed at 450 nm in dichloromethane is considerably stronger ($\epsilon = 7800$ M^{-1} cm^{-1}). None of the three copper(I) compounds **1**, **9**, and **10** show any detectable luminescence at room temperature, indicating that the electron withdrawing halide substituents in the bipyridine ligand cause intramolecular quenching of luminescence.

The absorption spectra of [Co^{II}(bpy-$Br_{0.5}Cl_{1.5}$)(ClBr)] (**11**) and [Ni^{II}(bpy-$Br_{0.46}Cl_{1.54}$)(H_2O)($Cl_{0.73}Br_{1.27}$)] (**12**) in acetonitrile are shown in Figure S6 of the Supporting Information. The olive green nickel(II) complex (**12**) has been shown to be of distorted square pyramidal geometry, whereas the deep blue cobalt(II) complex (**11**) seems to have a tetrahedral geometry. Indeed, as expected for tetrahedral cobalt (II) complexes, a structured strong intensity band with the peaks at 575 and 670 nm ($\epsilon = 430$ M^{-1} cm^{-1}) is observed in the visible region, which is attributed to $^4A_2 \rightarrow {}^4T_1(P)$ transition. In the NIR region, a weak shoulder at ~1000 nm ($\epsilon \approx 10$ M^{-1} cm^{-1}) and a relatively stronger band observed at 1350 nm ($\epsilon = 60$ M^{-1} cm^{-1}) are due to $^4A_2 \rightarrow {}^4T_1(F)$ and $^4T_2$ transitions, respectively. In high-spin square pyramidal nickel(II) complexes, splitting of the d-orbitals occur in the same way as tetragonally distorted six-coordinate nickel(II) complexes with weak axial field.[60] For such systems, B_{1g} is considered as the ground state. Accordingly, the four

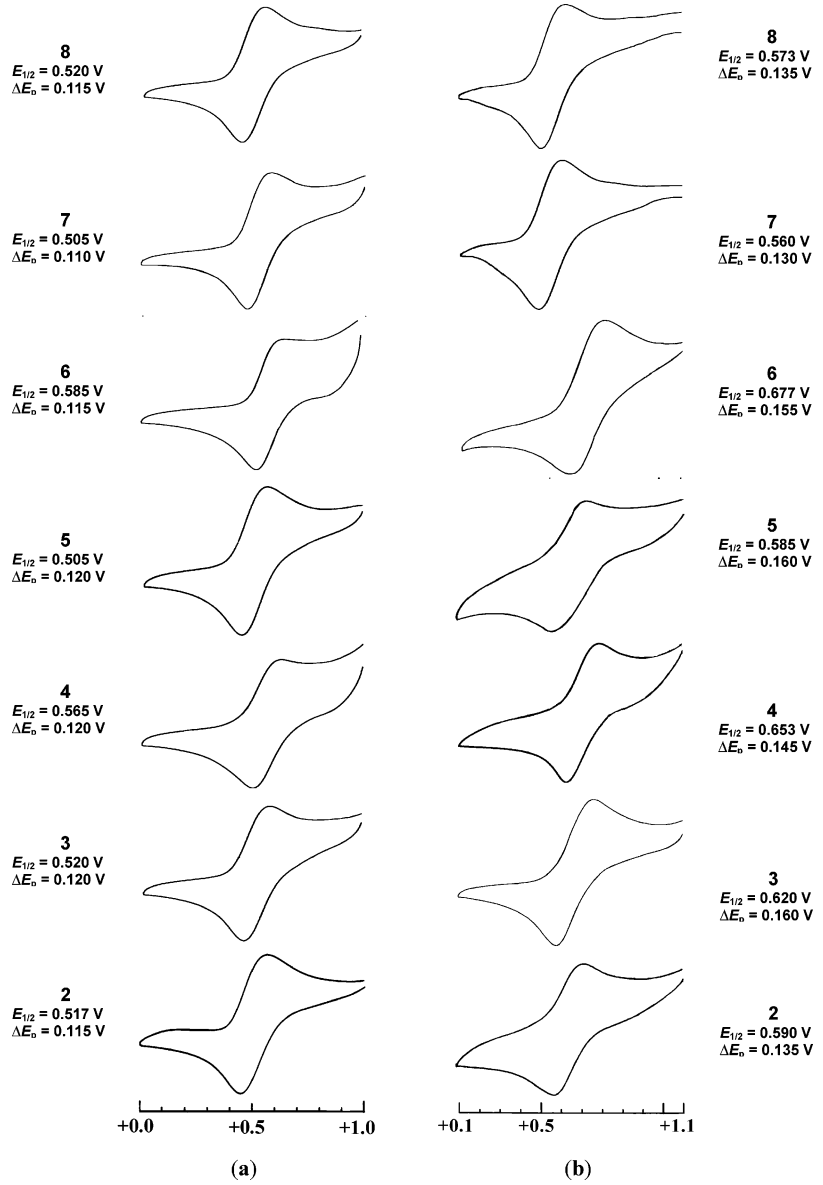

Figure 9. Cyclic voltammograms of [Cu(bpy-$Br_{2-x}Cl_x$)$Cl_{2-y}Br_y$] (**2**−**8**) in (**a**) acetonitrile (**b**) dichloromethane with a scan rate of 100 mV s^{-1}.

absorption bands observed in the visible-NIR region for **12** at 510 nm (ϵ = 125 M^{-1} cm^{-1}), 610 nm sh ($\epsilon \approx$ 10 M^{-1} cm^{-1}), 860 nm (ϵ = 30 M^{-1} cm^{-1}), and 1000 nm (ϵ = 60 M^{-1} cm^{-1}) may be assigned to the transitions from B_{1g} to $^3A_{2g}$ and ^3E_g(P), ^3E_g, A_{2g}, and $^3B_{2g}$ levels.

Electrochemical Measurements. The redox behavior of the copper complexes **1**−**10** have been studied in acetonitrile and in dichloromethane (except for complexes **9** and **10**, which are not soluble in dichloromethane) by cyclic voltammetric (CV) and Osteryoung square wave voltammetric (OSWV) measurements. The relevant electrochemical data ($E_{1/2}$ and ΔE_p values) of the compounds are listed in Table 6. The cyclic voltammograms of $[Cu^I(bpy\text{-}Br_2)_2]^+$ ($\mathbf{1}^+$) in the two solvent are compared in Figure S7. In acetonitrile, the oxidation of $\mathbf{1}^+$ occurs quasi-irreversibly (ΔE_p = 105 mV) at $E_{1/2}$ = 0.99 V, while in dichloromethane the electrochemical response is nearly reversible in nature (ΔE_p = 75 mV) with $E_{1/2}$ = 1.22 V. The high $E_{1/2}$ value for the oxidation of $\mathbf{1}^+$ is due to strong steric interaction between the CH_2Br moieties of the two bpy-Br_2 ligands when the oxidized bis-copper(II) complex tries to achieve its natural preference for planer configuration. The difference of the $E_{1/2}$ values of $\mathbf{1}^+$ by 0.23 V in the two solvents is a noteworthy feature. It appears that in a coordinating solvent like acetonitrile, the oxidized copper(II) species gets solvated, but not in a poorly coordinating solvent as dichloromethane. As a result, the solvated copper(II) species gets stabilized at a relatively less positive potential by achieving a five-coordinated geometry.[20]

The cyclic voltammograms of all of the copper(II) complexes **2**−**8** in acetonitrile and dichloromethane are shown in Figure 9 for comparison, and the corresponding electrochemical data are listed in Table 6. It may be noted that for each of the compounds, the $E_{1/2}$ values of the Cu^{II}/Cu^I couple is more positive in dichloromethane compared to that in acetonitrile and the average difference in $E_{1/2}$ values is about 80 mV. Further, the ΔE_p values of these compounds are relatively greater in dichloromethane (135-165mV) than

in acetonitrile (110−120mV). Clearly, the reduction of the copper(II) complexes having flattened tetrahedral geometry are more facile in a noncoordinating solvent as dichloromethane. However, partial solvation of the copper(II) complexes in acetonitrile helps to remove geometrical strain.

The data given in Table 6 also reveal that the copper(II) complexes containing metal-coordinated bromides have more positive $E_{1/2}$ values relative to their chloride bonded analogues. Thus, the $E_{1/2}$ values of [Cu(bpy-Cl_2)Br_2] (**6**) is 0.585 V in acetonitrile and 0.677 V in dichloromethane, while the corresponding values of [Cu(bpy-Cl_2)Cl_2] (**7**) in the two solvents are 0.520 and 0.573 V, respectively. This is expected because the copper(II) center becomes more electron-rich when it is coordinated with chloride ions than with bromide. Consequently, it is easier to add electrons (that is, reduction) to the bromide-coordinated compound, and hence the $E_{1/2}$ value of **6** is more positive than to that of **7**. Further, the $E_{1/2}$ values of [Cu(bpy-Br_2)Cl_2] (**5**) and [Cu(bpy-Cl_2)Cl_2] (**7**) are closely similar, indicating that rather than the substituents in the bipyridine ligands, the metal-bound halides control the redox potentials decisively. In the halogen-exchanged compounds **2**−**4**, the redox potentials increase in the order **2** < **3** < **4**, which is also the order of replacement of coordinated chloride by bromide.

The cyclic voltammograms of the dinuclear copper(I) complexes [Cu_2(bpy-$Br_{0.70}Cl_{1.30}$)$_2$(μ-Br)$_2$] (**9**) and [Cu_2(bpy-Br_2)$_2$(μ-Br)$_2$] (**10**) (Figure S8 of the Supporting Information) show that in both cases, electron transfer to the two identical metal centers take place simultaneously. The $E_{1/2}$ values of the two compounds 600 mV (**9**) and 610 mV (**10**) are practically same. The broad nature of the redox peaks indicates that following oxidation probably splitting of the bromide bridge takes place.

Conclusions

The ligands 6,6′-bis(bromo/chloromethyl)-2,2′-bipyridines bpy-Br_2 and bpy-Cl_2 have been used to address several issues, such as influence of the bulky substituents on the stereochemistry of complexes, intramolecular halogen exchange, and scrambling involving metal−halogen and carbon−halogen bonds, and photoinduced reduction of copper(II) complex to dimeric copper(I) complex.

Complex [Cu(bpy-Br_2)$_2$](ClO_4) (**1**) has been obtained as in two crystallographic modifications both of which exhibit almost ideal D_{2d} symmetry. In both forms, intermolecular C−H···O hydrogen bondings are involved, albeit in different ways. The redox potential of the Cu^I/Cu^{II} couple in **1** differs markedly in dichloromethane (1.22 V) and acetonitrile (0.99 V).

A number of halogen-exchanged and scrambled products have been isolated by reacting bpy-Br_2 with the hydrated chlorides of copper(II), cobalt(II), and nickel(II). The molecular structures of [Cu^{II}(bpy-$Br_{1.86}Cl_{0.14}$)($Cl_{1.89}Br_{0.11}$)] (**2**), [Cu^{II}(bpy-$Br_{0.63}Cl_{1.37}$)($Cl_{0.54}Br_{1.46}$)] (**4**), and [Cu^{II}(bpy-Cl_2)-Cl_2] (**7**) reveal flattened tetrahedral geometry, while the structures of the 5-coordinate compounds [Cu^{II}(bpy-$Br_{1.81}$-$Cl_{0.19}$)($Cl_{1.70}Br_{0.30}$)(H_2O)] (**3**) and [Ni^{II}(bpy-$Br_{0.46}Cl_{1.54}$)($Cl_{0.73}$-$Br_{1.27}$)(H_2O)] (**12**) show distorted to near-perfect square pyramidal geometry (τ = 0.25 for **3** and 0.01 for **12**). However, [Co^{II}(bpy-$Br_{0.50}Cl_{1.5}$)(ClBr)] (**11**) has been characterized as a tetrahedral compound. By following the course of reaction spectrophotometrically between bpy-Br_2 and $CuCl_2$·$2H_2O$ in acetonitrile at 45 °C for 7 h, a mechanism for halogen exchange/scrambling has been proposed. The redox behavior of the above copper(II) complexes as well as of [Cu^{II}(bpy-Br_2)Cl_2] (**5**) and [Cu^{II}(bpy-Cl_2)(Br_2)] (**6**) show solvent dependence and the compounds richer with metal-coordinated bromides exhibit more positive $E_{1/2}$ values.

The dinuclear copper(I) complexes [{Cu^I(bpy-$Cl_{1.30}Br_{0.70}$)-(μ-Br)}$_2$] (**9**) and [{Cu^I(bpy-Br_2)(μ-Br)}$_2$] (**10**) have been obtained by reacting $CuBr_2$ with bpy-Cl_2 and bpy-Br_2 at elevated temperature in the presence of light. From spectrophotometric studies, it has been established that the formation of the copper(I) complexes **9** and **10** does not take place in absence of light. Photoinduced homolytic cleavage of a Cu^{II}−Br bond of the precursor copper(II) complexes followed by dimerization lead to the formation of the bromo-bridged dicopper(I) complex species.

Acknowledgment. M.G. and P.B. are thankful to the Council of the Scientific and Industrial Research, India for the award of research fellowship.

Supporting Information Available: X-ray crystallographic files in CIF format for compounds **1a**, **1b**, **2**, **3**, **4**, **7**, **9**, and **12** and Figures S1−S8 (PDF). This material is available free of charge via the Internet at http://pubs.acs.org.

IC7014786